Magnetic Exchange Interactions in Perovskite Solid Solutions. Part 5.* The Unusual Defect Structure of $SrFeO_{3-y}$†

Terence C. Gibb
Department of Inorganic and Structural Chemistry, The University, Leeds LS2 9JT

A major investigation of the oxygen-deficient perovskite phase $SrFeO_{3-y}$ ($0.15 < y < 0.25$) has been carried out using ^{57}Fe Mössbauer spectroscopy, *X*-ray powder diffraction, and magnetic susceptibility measurements. The Mössbauer spectra have been recorded for a variety of samples at many temperatures in the range 4.2—900 K, and are extremely complex. Evidence has been found for three chemically distinct types of iron below 550 K, but above this temperature a thermally activated electron-transfer process takes place which results in a single narrow resonance. It is shown that ordering of oxygen vacancies can take place to a degree which depends upon both the thermal history and the oxygen content of a given sample. The magnetic properties are very unusual, and it is believed that aggregation of oxygen vacancies produces layers of tetrahedrally co-ordinated Fe^{3+} cations which show two-dimensional long-range order below 220 K. It is tentatively proposed that in the idealised structure of $SrFeO_{2.75}$ electron delocalisation can occur in the intervening layers which contain two distinct types of iron atom in octahedral co-ordination. The model leads to a plausible explanation for the observed disproportionation which occurs for $y > 0.28$.

The perovskite $SrFeO_3$ is of unusual interest, not only because it is one of the few oxide phases to contain iron in the +4 oxidation state, but also because it can be oxygen deficient. The early studies on this phase were superseded by major investigations of the Mössbauer spectroscopic properties[1] and electric and magnetic properties.[2] The perovskite phase was found to exist over the range $SrFeO_{3-y}$ ($0 \leqslant y \leqslant 0.28$), although compositions with $y < 0.14$ can only be made under high partial pressure of oxygen. Stoicheiometric $SrFeO_3$ is cubic, antiferromagnetic below a Néel temperature of $T_N = 130$ K, and shows metallic conduction. Oxygen deficiency leads to a tetragonal distortion of the unit cell, a decrease in Néel temperature, and an increase in resistivity. Attempts to reduce the oxygen content below that of $SrFeO_{2.72}$ lead to the precipitation of the Fe^{3+} oxide $SrFeO_{2.5}$ (often referred to as $Sr_2Fe_2O_5$). Subsequent work showed the existence of oxidation states of iron greater than +3 in the related strontium–iron phases $Sr_{1-x}La_xFeO_3$ ($0 \leqslant x \leqslant 1$)[3] and $Sr_3Fe_2O_{7-y}$ ($0 \leqslant y \leqslant 1$).[4]

Neutron diffraction data for $SrFeO_3$ have shown that the magnetic phase has an unusual helical spin arrangement.[5] A similar magnetic structure has also been described[6] for oxygen-deficient $SrFeO_{2.9}$. A neutron diffraction study of $SrFeO_{2.5}$ has revealed some disorder in the structure, but the atomic positions and magnetic spin directions are known to a good approximation.[7] A study of the perovskite phase using *X*-ray and electron diffraction techniques[8,9] has revealed some evidence for an ordered superstructure at $SrFeO_{2.75}$. The structure which was tentatively proposed features ordered oxygen vacancies with half of the iron atoms in six-co-ordination and half in five-co-ordination.

The corresponding barium phase $BaFeO_{3-y}$ is also known,[10] but cannot be compared directly with its strontium analogue because instead of being a cubic perovskite it has a related hexagonal structure. However, $CaFeO_3$ is a cubic perovskite and has excited particular interest because of a novel charge disproportionation at low temperatures which has been represented[11] as $2Fe^{4+} \longrightarrow Fe^{3+} + Fe^{5+}$. This has prompted a large number of studies of solid solutions, which will be referred to in the Discussion section. More importantly, it has resulted in a successful attempt[12,13] to stabilize six-co-ordinated Fe^{5+} in the perovskite La_2LiFeO_6.

The present work was initiated accidentally during studies of the solid solution $SrFe_{1-x}Sn_xO_{3-y}$ ($0 \leqslant x \leqslant 0.7$) which will be described separately in a later paper. As part of this programme a sample of the end member of the phase, $SrFeO_{3-y}$, was prepared and found to be inconsistent with published data. The subsequent investigation using Mössbauer spectroscopy, *X*-ray powder diffraction, and magnetic susceptibility measurements has revealed much new structural information, and has resulted in the proposal of a novel defect structure which contradicts previous suggestions.

Experimental

Samples of $SrFeO_{3-y}$ were prepared from accurately weighed amounts of spectroscopic grade α-Fe_2O_3 and $SrCO_3$, ground together in a ball mill, pressed into a pellet, and fired in air at high temperature. Various heat treatments were employed to give a total of eleven samples.

Initial characterization in each case was by *X*-ray powder diffraction recorded with a Philips diffractometer using nickel-filtered Cu-K_α radiation. With the exception of sample (**1e**), all samples gave a simple pattern from a perovskite lattice with a very small tetragonal distortion and no unattributable lines. No attempt was made to identify any very small changes in the lattice parameters because of the difficulty in eliminating minor systematic errors, and the very small splittings involved. The cell constants for sample (**1a**) were $a = 3.866$ and $c = 3.852$ Å in good agreement with earlier work.[8]

Chemical analysis was carried out to determine the oxygen deficiency. The Sr:Fe ratio was assumed to be exactly 1:1, and the proportion of iron in oxidation states greater than +3 was estimated by digestion of a weighed aliquot in a standardised solution of ammonium iron(II) sulphate, followed by addition of HCl and titration with cerium(IV) sulphate using ferroin as indicator. Each analysis was performed in duplicate together with a calibrating blank. The value of y in the formula $SrFeO_{3-y}$ was then calculated to within an estimated accuracy of ± 0.005. The results obtained were in good agreement with previously published values, and were also consistent with the spectroscopic data.

* Part 4, T.C. Gibb, *J. Chem. Soc., Dalton Trans.*, 1984, 667.

† *Non-S.I. units employed:* Torr ≈ 133 Pa, B.M. = 9.274×10^{-24} J T^{-1}.

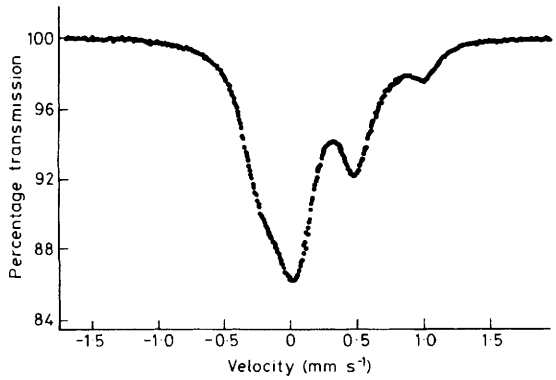

Figure 1. The ^{57}Fe Mössbauer spectrum at 295 K of sample (**1a**) ($SrFeO_{2.844}$)

The oxygen content and the spectroscopic properties were found to be very dependent on the heat treatment given to a particular sample, and therefore these are described in full detail.

Sample (**1a**): $SrCO_3$ + α-Fe_2O_3 preheated to 1 200 K for 17 h, followed by heating to 1 510 K for 5 d, regrinding, and heating to 1 530 K for 6 d. The final cooling was carried out in the furnace with a cooling time from 1 250 to 750 K of *ca.* 310 min (*ca.* 1° min^{-1} at 750 K). Chemical analysis gave $SrFeO_{2.844}$.

Sample (**1b**): sample (**1a**) re-annealed at 700 K *in vacuo* (10^{-4} Torr) for 1 d (after similar periods at lower temperatures). Chemical analysis gave $SrFeO_{2.808}$.

Sample (**1c**): sample (**1a**) re-annealed at 700 K in air for 5 d and then slowly cooled as above. Chemical analysis gave $SrFeO_{2.846}$.

Sample (**1d**): sample (**1a**) re-annealed at 890 K in air for 5 d and then slowly cooled as above. Chemical analysis gave $SrFeO_{2.838}$.

Sample (**1e**): sample (**1a**) annealed at 900 K *in vacuo* (10^{-4} Torr) for 3 d (after similar periods at lower temperatures) and cooled quickly to room temperature. Chemical analysis gave $SrFeO_{2.589}$.

Sample (**2a**) a repeat preparation from $SrCO_3$ + α-Fe_2O_3 similar to sample (**1a**) with preheating at 1 200 K for 24 h, 1 580 K for 4 d, regrind, 1 580 K for 5 d, followed by slow cooling in the furnace as for sample (**1a**). Chemical analysis gave $SrFeO_{2.838}$.

Sample (**2b**): sample (**2a**) reheated to 1 200 K for 24 h, and then quenched to room temperature in *ca.* 1 min. Chemical analysis gave $SrFeO_{2.760}$.

Sample (**2c**): sample (**2a**) re-annealed at 700 K *in vacuo* (10^{-4} Torr) for 5 d. Chemical analysis gave $SrFeO_{2.749}$.

Sample (**2d**): sample (**2a**) annealed at 1 570 K for 24 h and then cooled very slowly at an average rate of *ca.* 3° h^{-1} down to 680 K. Chemical analysis gave $SrFeO_{2.804}$.

Sample (**2e**): sample (**2d**) reheated to 1 200 K for 24 h and then cooled more quickly, reaching 750 K in 18 min (*ca.* 10° min^{-1} at 750 K). Chemical analysis gave $SrFeO_{2.787}$.

Sample (**3**): a third preparation from $SrCO_3$ + α-Fe_2O_3, with no preheating and only one heating cycle to 1 500 K for 6 d followed by the same cooling as for sample (**1a**). Chemical analysis gave $SrFeO_{2.809}$.

Mössbauer spectra were recorded for absorber temperatures in the range 4.2—900 K with a ^{57}Co/Rh source matrix at room temperature; isomer shift values are relative to the spectrum of metallic iron. Temperatures below 80 K were obtained using liquid helium in an Oxford Instruments CF500 Continuous Flow Cryostat controlled by a DTC2 Digital Temperature Controller. From 80 K to room temperature a Ricor Variable Temperature Cryostat MCH-5B was used, and above room temperature a Ricor Furnace MF-2A, both controlled by a Ricor Temperature Controller TC-4B. The main spectrometer was based upon either an MS-102 Microprocessor by Cryophysics Ltd., or a Northern Scientific NS-900 multichannel analyser.

The majority of spectra were recorded using moderately thick absorbers to give a very high percentage absorption, but with some degree of saturation which usefully intensified the weaker lines. In cases where accurate area ratios of the components in a spectrum were required, the equivalent spectra were accumulated using absorbers reduced in thickness by a factor of *ca.* 10 and long counting times so that the normal saturation effects were reduced as much as possible. All data were processed using an Amdahl 470 computer.

Magnetic susceptibility data were collected for three samples in the temperature range 80—300 K using the Gouy method.

Results

In discussing the results which have been obtained, it is convenient in the first instance to describe the phenomena which have been observed, and to leave most of the discussion of the chemical significance of the results until later. In view of the many significant variations in the rather complicated Mössbauer spectra which have been recorded, it is necessary to illustrate these in considerable detail.

Sample (**1a**) ($SrFeO_{2.844}$).—The ^{57}Fe Mössbauer spectrum at 295 K of the first sample prepared, (**1a**), is illustrated in Figure 1. There are clearly three absorptions at *ca.* 0.0, 0.5, and 1.0 mm s^{-1} (relative to metallic iron), of which the most negative is evidently of compound shape. This result does not agree with the original data of Gallagher *et al.*[1] for a sample described as $SrFeO_{2.86}$ which only showed absorptions at *ca.* 0.0 and 0.5 mm s^{-1}. It was not immediately obvious as to whether the third component was a genuine property of the $SrFeO_{3-y}$ phase, or was evidence of a second phase present in the sample. Although the *X*-ray powder data showed no lines other than those of the tetragonally distorted perovskite lattice, the presence of an amorphous material could not be excluded. Further investigation was prompted by this discrepancy, resulting in the work described here.

It is interesting to note that Shimony and Knudsen[3] have reported data at 295 K for a sample of composition $SrFeO_{2.841}$ in which the third component is clearly visible but has been totally ignored in the data analysis. It is indeed possible that there is a weak component present in the original data of Gallagher *et al.*[1] which is less apparent because of the comparatively small number of data points in the region of interest.

The correct analysis of the spectrum was only discovered as the result of Mössbauer measurements made at higher temperatures in an evacuated furnace. The spectrum of sample (**1a**) at 400 K (Figure 2) measured over a period of 3 d shows no significant change, and even at 500 K (for 2 d), the slight blurring of the spectrum can be easily overlooked. However, at 600 K (for 1 day) the structure of the spectrum has largely collapsed, although the linewidth of 0.67 mm s^{-1} further reduces at 700 K (for 1 d) to 0.45 mm s^{-1}. The single component at 700 K is close to the weighted mean of the low-temperature spectra (after allowing for the thermal shift). This is strong evidence that all components of the spectrum in Figure 1 belong to a single-phase material which undergoes a thermally activated electron-exchange process at high temperature, the frequency of which is *ca.* 10^7 s^{-1} at 550 K. In this context it can be noted that the intermediate spectra are broadly consistent with those of spinel oxides in which a thermally activated electron exchange

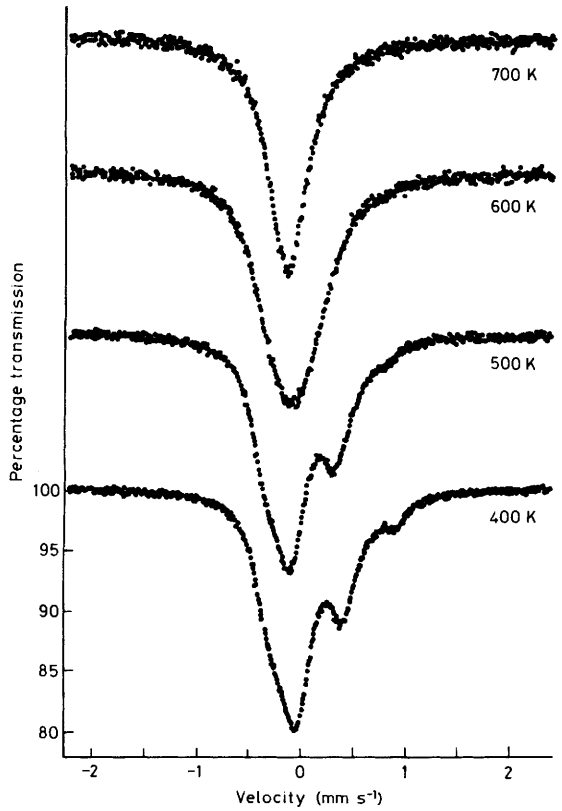

Figure 2. The ^{57}Fe Mössbauer spectrum at 400, 500, 600, and 700 K of sample (**1a**) ($SrFeO_{2.844}$) *in vacuo*. Note the gradual collapse of the spectrum above 500 K indicating a thermally activated electron-exchange process

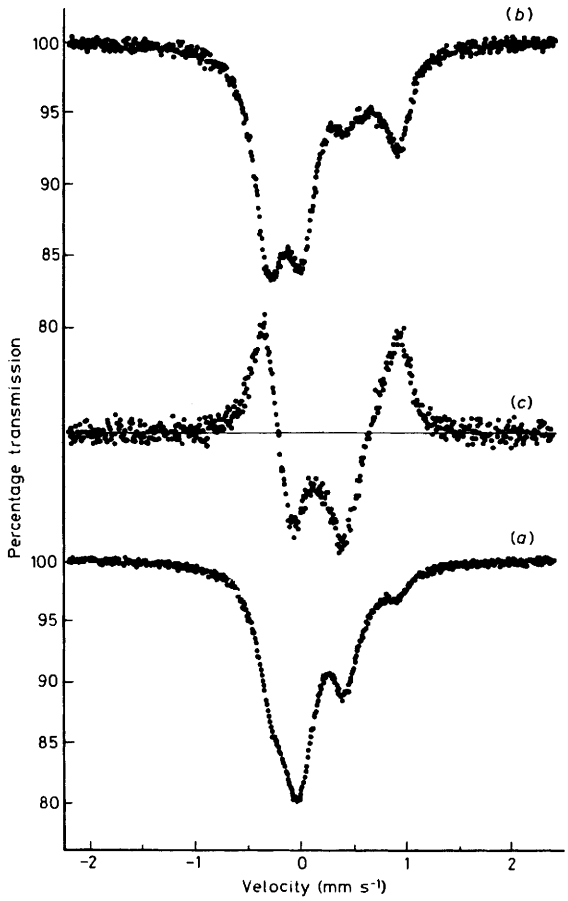

Figure 3. The ^{57}Fe Mössbauer spectrum of sample (**1a**) ($SrFeO_{2.844}$) (*a*) at 400 K (before heating to 700 K) and (*b*) at 400 K (after heating to 700 K). The difference spectrum (*c*) reveals the existence of two related pairs of lines

between Fe^{2+} and Fe^{3+} ions is taking place.[14] The nature of the valence states 'frozen' out at lower temperatures in the present case will be discussed later.

The sample was now cooled by successive stages to 550 K (3 d), 500 K (1 d), 400 K (1 d), and 300 K (1 d) before exposing to air again. It was immediately evident that the heating cycle was not fully reversible, that exposure to air at 300 K had no effect, and that a major change had occurred which was subsequently shown to involve loss of oxygen. The final material is designated sample (**1b**), and gave an analysis of $SrFeO_{2.808}$. However, a second sample of (**1a**) was taken through several heating cycles to 700 K with intermediate periods at 550 K for detailed measurement of the Mössbauer spectrum. Each period of heating (cooling) was completed within 10 min. After 10 min at 700 K (during which time it was established that the Mössbauer spectrum had indeed collapsed to a single line), the spectrum at 550 K showed no observable change. Only a slight change was observed after 65 min, a substantial change after 425 min, while the final spectrum after 80 h was similar to that of sample (**1b**). It has therefore been established that the electron-exchange process can take place in $SrFeO_{2.844}$ at 700 K *independently* of oxygen loss, which is a comparatively slow process at this temperature. Moreover, the electron-exchange process takes place over a wide range of oxygen content.

One important feature of the heating cycle which converted sample (**1a**) into (**1b**) was that all experimental variables were kept constant except the temperature, *i.e.* the absorber, furnace geometry, and detection system remained invariant. Therefore, it became possible to subtract data (normalised to the same baseline) at identical temperatures during the heating and cooling stages, and thus to obtain a true difference spectrum. This is illustrated in Figure 3 for data obtained at 400 K. The unidentified absorption at *ca.* 0.8 mm s^{-1} in sample (**1a**) has increased substantially in intensity, but there is an equivalent increase in absorption at *ca.* −0.4 mm s^{-1} which can be attributed to the second component of a symmetrical quadrupole doublet. The component at *ca.* 0.4 mm s^{-1} has decreased in intensity, with an equivalent decrease at *ca.* −0.1 mm s^{-1} which can be attributed to the second component of a further quadrupole doublet. This direct evidence for the positions of related quadrupolar components in the spectrum was used to compute various models for the spectra of samples (**1a**) and (**1b**).

The final result is a model in which there are three quadrupole doublets which for the present will be identified as X, Y, and Z. Furthermore, this overall interpretation has been found to give a reasonable analysis for nearly all of the paramagnetic spectra which have been obtained from samples of $SrFeO_{3-y}$, and to be compatible with the magnetic spectra at low temperatures. A typical spectral analysis is indicated in Figure 4 for sample (**1a**) at 220 K. In general, it is considered that the calculated values for the isomer shifts (δ), quadrupole splittings (Δ), and linewidths (Γ) are reasonably precise (± 0.01 mm s^{-1}). However, the calculated area ratios are unlikely to be more accurate than $\pm 2\%$, because the model assumes all six lines to be symmetrical Lorentzian profiles, *i.e.* no allowance is made for minor variations in shift and splitting which can be reasonably expected in a solid solution with a randomised environment.

Table 1. Calculated Mössbauer parameters for sample (**1a**)

Component	δ/mm s^{-1}	Δ/mm s^{-1}	Γ/mm s^{-1}	Area (%)
X	0.36	1.26	0.24	9
Y	0.27	0.46	0.31	45
Z	−0.06	0.19	0.32	46

Table 2. Parameters from the Mössbauer spectrum of sample (**1a**)

Component	B/T	δ/mm s^{-1}	ε/mm s^{-1}
X	45.6	+0.43	−0.68
Y	44.1	+0.36	~0
Z	29.3	+0.03	~0

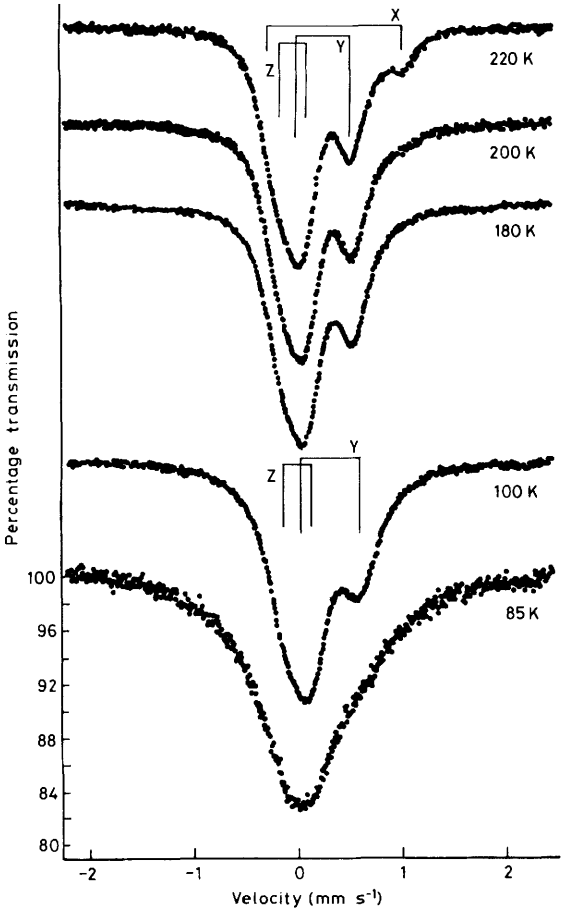

Figure 4. The ^{57}Fe Mössbauer spectra of sample (**1a**) ($SrFeO_{2.844}$) at 85, 100, 180, 200, and 220 K. Note the 'disappearance' of the X component below 220 K, and the onset of magnetic broadening at 85 K

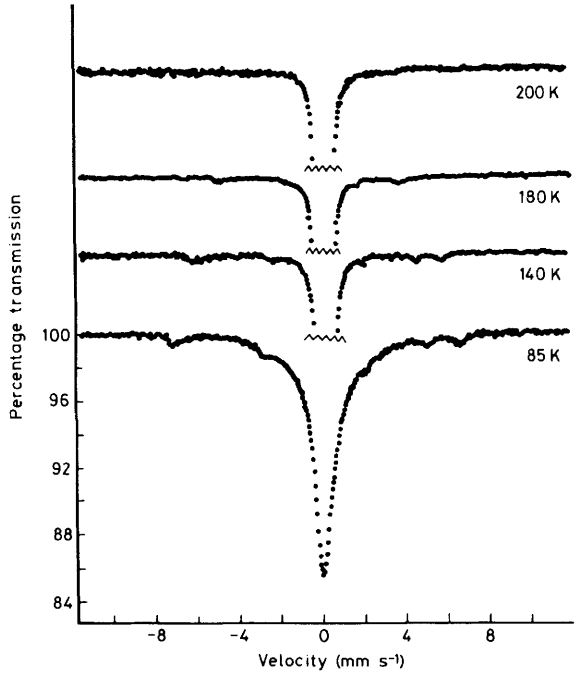

Figure 5. The ^{57}Fe Mössbauer spectrum of sample (**1a**) ($SrFeO_{2.844}$) at 85, 140, 180, and 200 K with a wider velocity scan than in Figure 4. Note the existence of a magnetic hyperfine pattern at 85 K which collapses with increase in temperature

The calculated parameters for a 'thin' absorber of sample (**1a**) at 295 K are as in Table 1. High-temperature measurements at 800 and 900 K *in vacuo* are referred to under sample (**1e**).

Selected spectra for sample (**1a**) in the temperature range 85—220 K are shown in Figure 4. The spectrum shows no significant change between 220 and 295 K other than the expected thermal shifts, but below 220 K the X component of the spectrum 'disappears'. Between 100 and 180 K it is possible to analyse the spectra in terms of two quadrupole doublets, Y and Z, in the same relative ratios as in the high-temperature spectra. At 85 K, substantial broadening has appeared, which can safely be assumed to be of magnetic origin. This spectrum is closely equivalent to published data[1] for $SrFeO_{2.86}$. The reason for the 'disappearance' of the X component was discovered by remeasuring some of the spectra on a wider velocity scan as shown in Figure 5. It can be seen that there is now a magnetic hyperfine pattern at 85 K which collapses with increase in temperature. The poor definition of this component above 180 K suggests that there is either relaxation narrowing or a spread of hyperfine field values.

Mössbauer spectra for sample (**1a**) at 4.2, 20, 40, and 60 K are shown in Figure 6. The spectrum at 4.2 K shows considerable similarity to the earlier published data,[1] although the increased number of data points plotted here show clearly that there are at least three magnetic components which have been identified as X, Y, and Z. The X component is easily equated with the magnetic splittings in Figure 4, and the Y and Z components are similar to those identified earlier.[1] All attempts to computer fit this spectrum with three magnetic hyperfine splittings failed, and it was evident that there was an excess of absorption intensity in the central region of the spectrum. Examination of the spectra at 20, 40, and 60 K shows a substantial increase in the central absorption by an inward collapse of the Y and Z components in a manner strongly suggestive of relaxation effects. It is therefore believed that the spectrum at 4.2 K is not a completely static spectrum, but is already partially collapsed even at this low temperature. Measurements below 4.2 K would be useful in verifying this, but were not possible with the croystat used. The parameters which describe the stick diagrams are the magnetic flux density (B), isomer shift (δ), and the quadrupole perturbation parameter (ε). The last is obtained from the positions of the outer four lines as $\varepsilon = \frac{1}{4}[(d - c) - (b - a)]$. The estimated numerical values for the static hyperfine splittings are given in Table 2. Unfortunately, it is not

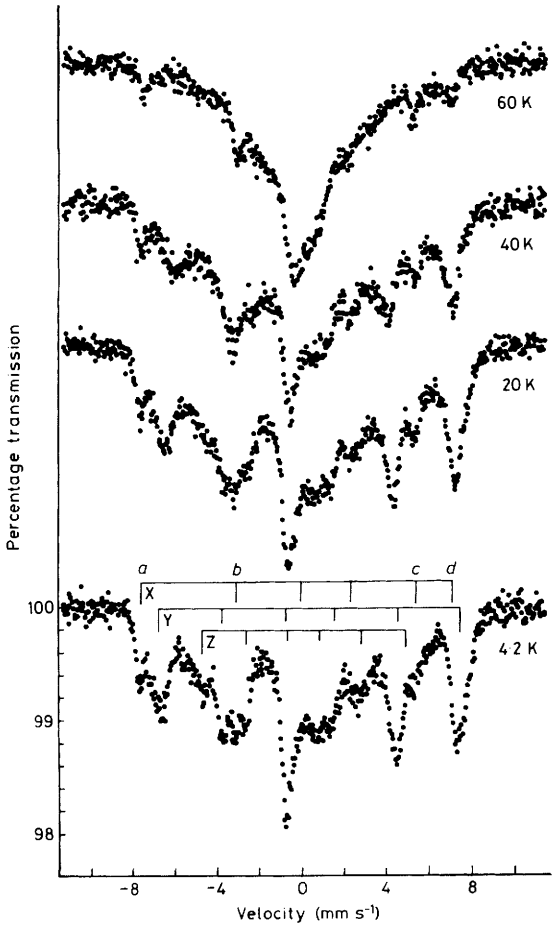

Figure 6. The ^{57}Fe Mössbauer spectrum of sample (**1a**) ($SrFeO_{2.844}$) at 4.2, 20, 40, and 60 K. A suggested assignment of the lines from the X, Y, and Z components at 4.2 K is indicated. Note the increase in intensity in the centre of the spectrum with rise in temperature, indicating the presence of relaxation effects

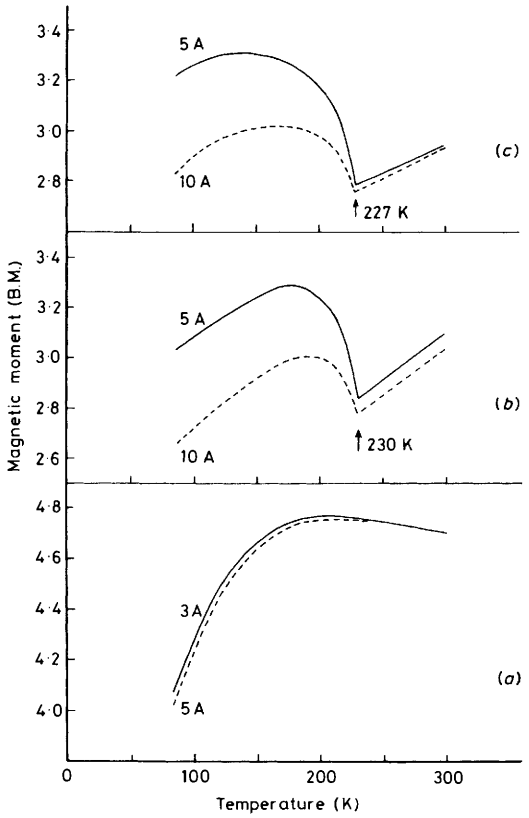

Figure 7. The effective magnetic moment per Fe atom in (*a*) sample (**1a**) ($SrFeO_{2.844}$) with magnet currents of 3 and 5 A, (*b*) sample (**2b**) ($SrFeO_{2.760}$) at 5 and 10 A, (*c*) sample (**2c**) ($SrFeO_{2.749}$) at 5 and 10 A. The differences in flux density $B_1^2 - B_2^2$ which correspond to a magnet current of 3, 5, and 10 A were 0.046, 0.118, and 0.301 T^2

possible to give a reliable estimate of the relative areas of the components.

The magnetic susceptibility data for sample (**1a**) were converted to values for the magnetic moment per Fe atom, and are plotted in Figure 7. The results are broadly in agreement with earlier work.[1] The magnetic moment is independent of the field at room temperature, but shows a slight field dependence below 200 K. The data for magnet currents of 3 A and 5 A are shown in Figure 7(*a*). There is no discernible discontinuity in the values for sample (**1a**) at *ca.* 220 K. The field dependence may indicate a parasitic magnetism due to spin misalignment or some defect-related phenomenon. The reduction in the magnetic moment per Fe atom below 220 K is consistent with antiferromagnetic interactions.

The computed isomer shift (δ) values for the three components X, Y, and Z as a function of temperature are shown in Figure 8 as filled circles. The cross symbols represent the isomer shift of the single-line spectrum above 550 K, the weighted mean of the whole spectrum between 220 and 550 K, and the weighted mean of only the Y and Z components below 220 K. The numbered open circles represent isomer shift values for other compounds which will be referred to in the Discussion section. Note that there is no discontinuity in the Y and Z isomer shifts at 220 K, but that the weighted mean is affected by omitting the X component. The trend towards more negative shift with increasing temperature is due to the second-order Doppler shift, but no attempt has been made to evaluate this effect numerically.

Table 3. Calculated Mössbauer parameters for sample (**1b**)

Component	δ/mm s^{-1}	Δ/mm s^{-1}	Γ/mm s^{-1}	Area (%)
X	0.36	1.32	0.23	30
Y	0.30	0.50	0.36	20
Z	−0.08	0.27	0.26	50

Sample (**1b**) ($SrFeO_{2.808}$).—The material obtained by annealing sample (**1a**) *in vacuo* at 700 K was subjected to a further detailed investigation at low temperatures. A selection of spectra between 85 and 295 K are shown in Figure 9. The spectra at 220 and 295 K are very similar to that at 400 K shown in Figure 3. The sharper resolution at 295 K may be a result of eliminating vibrational effects associated with the furnace/cryostat. The calculated parameters for a 'thin' absorber of sample (**1b**) at 295 K using the same three-component model are as in Table 3.

A comparison with Figures 1—8 for sample (**1a**) reveals a number of interesting points which appear to be valid for other samples also. As the oxygen content decreases, the X component increases substantially in intensity but remains sharp despite a small increase in the quadrupole splitting, Δ. The Y component decreases substantially in intensity but also broadens considerably with the result that the area ratios are more difficult to determine in the samples with low oxygen

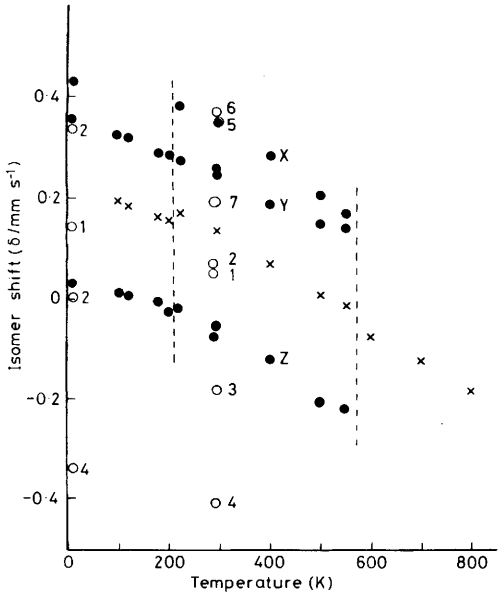

Figure 8. The isomer shift values (δ/mm s^{-1}) as a function of temperature for sample (**1a**): (●) X, Y, and Z components; (×) weighted mean of each spectrum. Note that some oxygen loss has taken place above 600 K. The weighted mean below 220 K refers only to the Y and Z components. The numbered circles represent other relevant compounds: (1) stoicheiometric $SrFeO_3$; (2) stoicheiometric $CaFeO_3$, which shows a single line at 295 K, but two different components at 4.2 K; (3) $SrLa_3LiFeO_8$ containing Fe^{4+} ($S = 2$); (4) La_2LiFeO_6 containing Fe^{5+} ($S = \frac{3}{2}$); (5) $EuFe_{0.5}Co_{0.5}O_3$ containing Fe^{3+} ($S = \frac{5}{2}$) in six-co-ordination; (6) $SrFeO_{2.5}$ containing Fe^{3+} in six-co-ordination; (7) $SrFeO_{2.5}$ containing Fe^{3+} in four-co-ordination

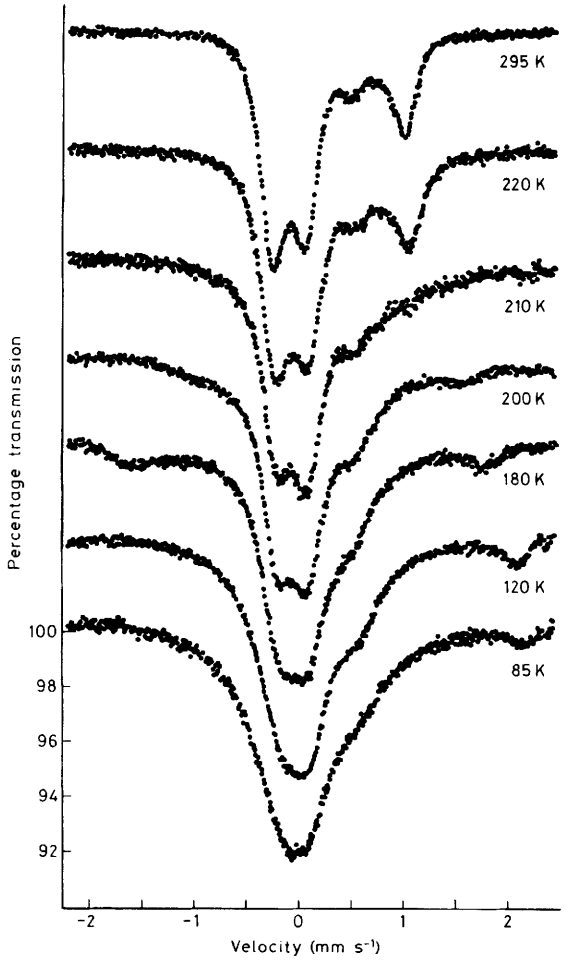

Figure 9. The ^{57}Fe Mössbauer spectrum of sample (**1b**) ($SrFeO_{2.808}$) at 85, 120, 180, 200, 210, 220, and 295 K. Note the appearance of lines from a magnetic hyperfine splitting below 220 K

content. Indeed, the lineshapes may no longer be Lorentzian or symmetrical and in particular this may affect the area calculation. The Z component always contributes *ca.* 48 ± 2% to the total spectrum area, but there is a small negative shift by −0.02 mm s^{-1} and a small increase in quadrupole splitting and linewidth. However, the most significant change is the growth of the X component at the expense of the Y component.

Below 220 K the X component develops into a magnetic hyperfine splitting as it did for sample (**1a**), but the increase in intensity means that the magnetic lines are now clearly visible. However, in this sample it appears that the central resonance (Y and Z components) does change slightly with temperature. It is possible that this is in effect a weak magnetic broadening induced by the magnetic X component, rather than a significant chemical change.

Similar spectra measured using a larger velocity scan are shown in Figure 10. Compared to Figure 5, the magnetic X component is much more prominent. It is also apparent that some inward broadening of the outer magnetic lines takes place with rise in temperature which together with intensity changes seems to indicate substantial relaxation narrowing.

The spectrum at 4.2 K in Figure 11 is remarkable in that the central resonance is still very intense and comparatively narrow. In comparison with the equivalent spectrum for sample (**1a**) in Figure 6, the X component is very sharp with no appreciable relaxation, but completely dominates the magnetic lines from Y and Z which can still be seen (*e.g.* at *ca.* −7 and −5 mm s^{-1} respectively) but are broadened and partly collapsed into the central resonance. This collapse continues with rise in temperature. Note that the baseline in all these magnetic spectra has been rigorously corrected for curvature arising from geometry effects by normalisation with a blank spectrum. The outer X lines remain at the same absolute intensity, but the grossly broadened Y and Z components collapse between 20 and 85 K.

The magnetic flux density of the hyperfine field of X has been measured by inspection in the various spectra, and is plotted as a function of temperature in Figure 12. The solid line represents the $S = \frac{5}{2}$ Brillouin function with $B(T = 0) = 46.1$ and $T_c = 220$ K. The hyperfine field is clearly consistent with a Brillouin behaviour, although it is difficult to be certain of the ordering temperature which in reality could be higher than 220 K.

Sample (**1c**) ($SrFeO_{2.846}$).—Published data[8] have suggested that oxygen loss from $SrFeO_{3-y}$ is only significant above 800 K, and therefore the considerable oxygen loss caused by annealing at 700 K *in vacuo* was surprising. It seemed possible that the relative intensity changes in the X and Y components occurred because of this oxygen loss. To investigate this further, an aliquot of sample (**1a**) was annealed at 700 K in air for 5 d and then slowly cooled. Chemical analysis of this sample, (**1c**), showed no loss of oxygen within experimental error.

However, the Mössbauer spectrum at 295 K (Figure 13) showed a significant increase in the intensity of the X component and an overall spectrum which was clearly intermediate between samples (**1a**) and (**1b**). The calculated parameters from the spectrum of a 'thin' absorber at 295 K are as in Table 4, these are clearly intermediate between the two earlier results.

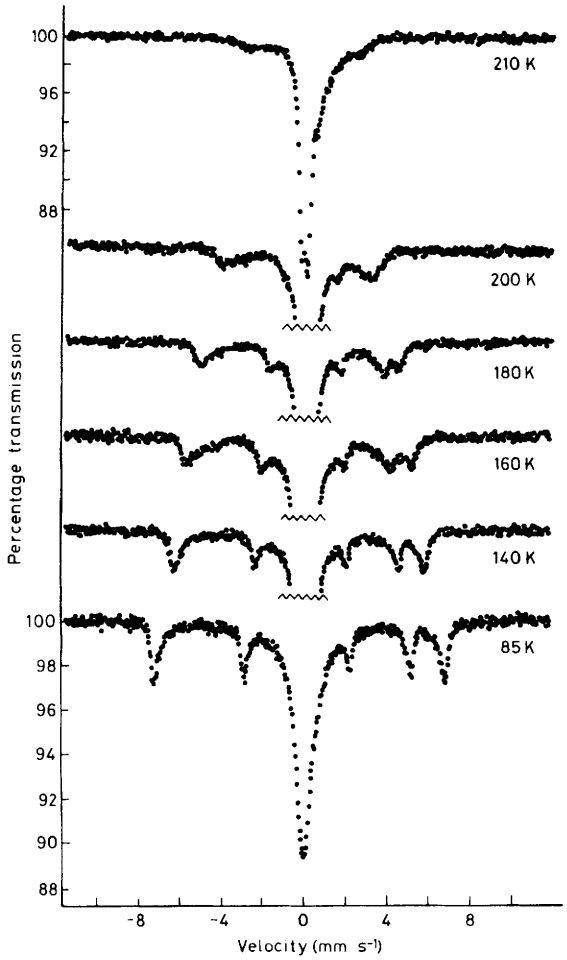

Figure 10. The ^{57}Fe Mössbauer spectrum of sample (**1b**) ($SrFeO_{2.808}$) at 85, 140, 160, 180, 200, and 210 K using a wider velocity scan than in Figure 9

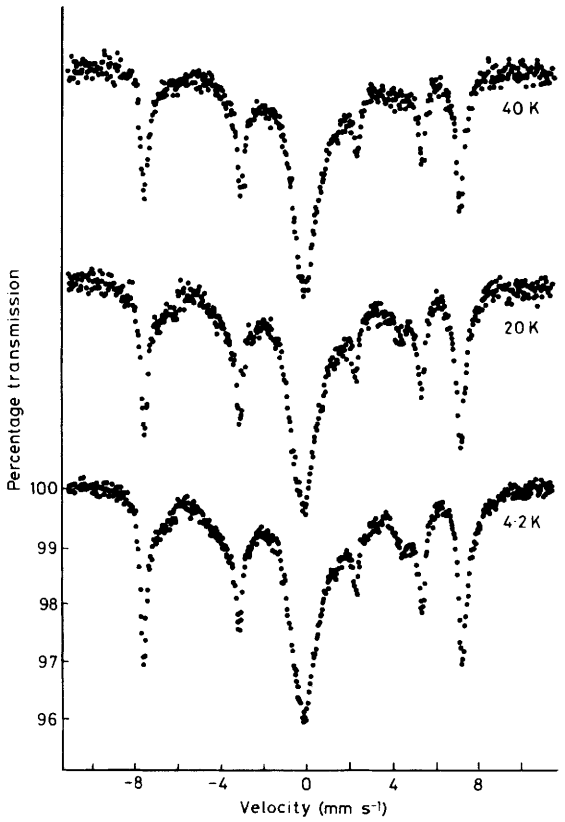

Figure 11. The ^{57}Fe Mössbauer spectrum of sample (**1b**) ($SrFeO_{2.808}$) at 4.2, 20, and 40 K

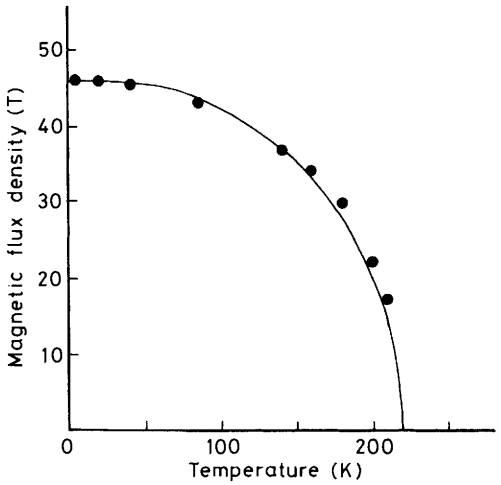

Figure 12. The magnetic flux density of the hyperfine field in sample (**1b**) as a function of temperature. The solid curve is the $S = \frac{5}{2}$ Brillouin function with an ordering temperature of 220 K

The primary deduction which can be made is that the defect structure of the solid depends not only on the oxygen content but also on its thermal history, a fact not previously established.

A decrease in temperature results once again in the magnetic splitting of the X component below *ca.* 210 K as can be seen in Figures 13 and 14. However, the spectrum at 180 K in Figure 14 shows much greater relaxation collapse than the equivalent spectrum for sample (**1b**) (Figure 10), and confirms the similar observations made for sample (**1a**). The spectrum of sample (**1c**) at 4.2 K (Figure 15) is intermediate between those for (**1a**) (Figure 6) and (**1b**) Figure 11. The Y and Z magnetic components are clearly visible, but are evidently not static even at 4.2 K, showing rapid collapse above 20 K, and are almost fully narrowed at 85 K. The low-temperature annealing in air of sample (**1a**) has thus resulted in a drastic change in the spectroscopic properties despite their being no significant loss of oxygen.

Sample (**1d**) ($SrFeO_{2.838}$).—Sample (**1d**) was made by annealing sample (**1a**) in air at 890 K for 5 d and then slowly cooling as before, the intention being to obtain a comparison with the similar annealing *in vacuo* which resulted in sample (**1e**). Rather surprisingly the spectrum at 295 K was very similar to that of the starting material. At 890 K substantial oxygen loss will occur,[8] and the fact that the cooling cycle below this temperature followed that for sample (**1a**) resulted in a very similar preparation which was not investigated further.

Table 4. Calculated Mössbauer parameters for sample (**1c**)

Component	δ/mm s^{-1}	Δ/mm s^{-1}	Γ/mm s^{-1}	Area (%)
X	0.36	1.31	0.21	18
Y	0.28	0.48	0.32	33
Z	−0.08	0.23	0.23	49

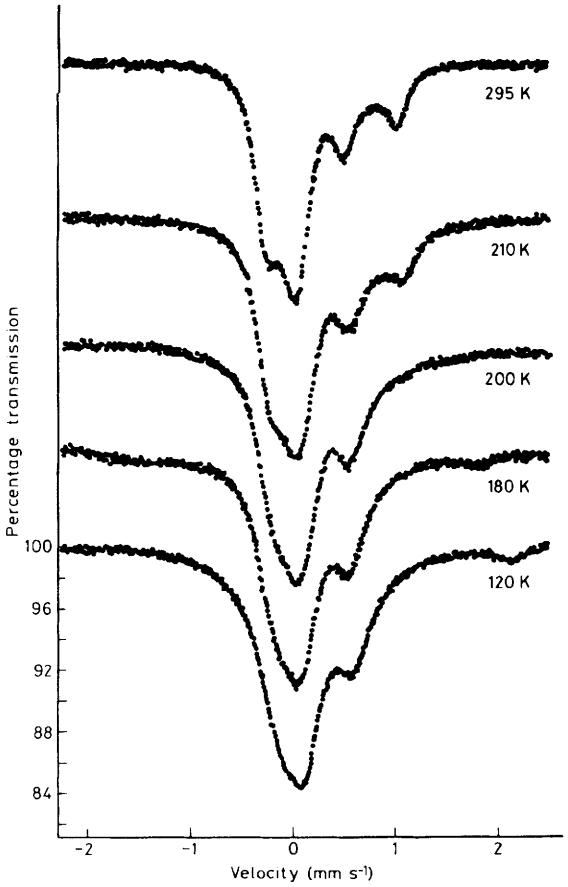

Figure 13. The ^{57}Fe Mössbauer spectrum of sample (**1c**) ($SrFeO_{2.846}$) at 120, 180, 200, 210, and 295 K. Note the appearance of lines from a magnetic hyperfine splitting below 210 K

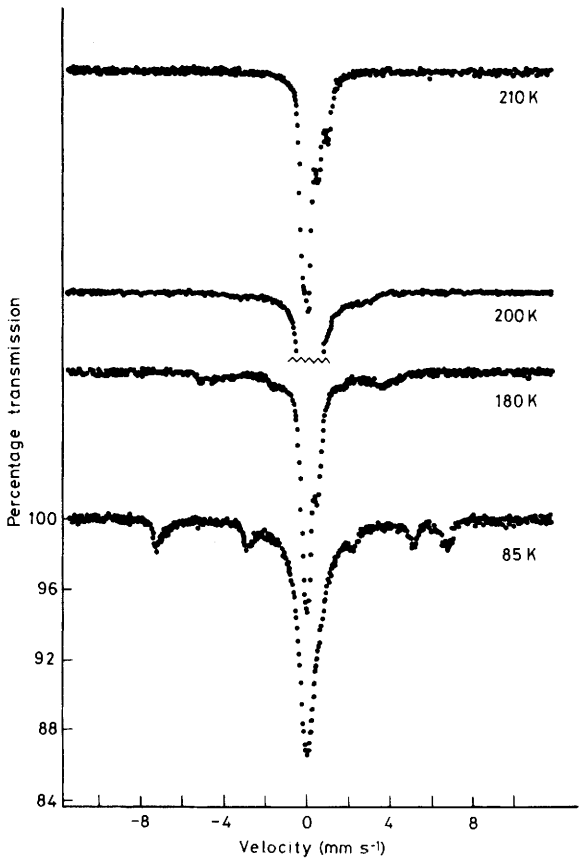

Figure 14. The ^{57}Fe Mössbauer spectrum of sample (**1c**) ($SrFeO_{2.846}$) at 85, 180, 200, and 210 K using a wider velocity scan than in Figure 13

Sample (**1e**) ($SrFeO_{2.589}$).—A further aliquot of sample (**1a**) was annealed *in vacuo* for varying periods. After 80 h at 700 K [as described earlier for sample (**1a**)], it was heated to 800 K for 1 d, and the spectrum recorded during that time is shown in Figure 16. At this juncture a further spectrum recorded at 550 K was similar to that for sample (**1b**) and suggested that the material was still single phase. A further 24 h at 900 K revealed broadened 'wings' to the spectrum which became more marked during the period 24—72 h. Further heating was precluded by a deterioration of the furnace at this temperature. The sample (**1e**) was then analysed and found to have lost more oxygen.

The spectrum at 295 K is shown in Figure 17. The two magnetic hyperfine splittings arise from the tetrahedral and octahedral Fe^{3+} sites[1] in $SrFeO_{2.50}$ which has a Néel temperature[7] of 700 K, and this phase was readily identifiable in the *X*-ray powder pattern together with some residual perovskite phase. Both Fe^{3+} sites show a large quadrupole splitting, and in the paramagnetic phase result in a broadened doublet which is evident in Figure 16. Other spectra were recorded for this two-phase sample, but are not reported here.

Sample (**2a**) ($SrFeO_{2.838}$).—A completely new preparation of $SrFeO_{3-y}$ was carried out using the same preparative technique and proved to be very similar to the original sample (**1a**). It is evident that the preparation is reproducible.

Sample (**2b**) ($SrFeO_{2.760}$).—An aliquot of sample (**2a**) was heated to 1 200 K in air for 24 h and then quenched to room temperature in *ca.* 1 min. Chemical analysis showed substantial loss of oxygen, and it had been anticipated that this sample would be inhomogeneous and probably two-phase. However, the *X*-ray powder pattern showed only perovskite lines, implying a very rapid take-up of oxygen. The magnetic susceptibility data are shown in Figure 7(*b*), and show a distinct discontinuity at 230 K. Below this temperature the data show marked field dependence, and the behaviour is very different to that of sample (**1a**). The average moment per Fe atom in the paramagnetic region is much lower than for sample (**1a**), despite nominal reduction from Fe^{4+} to Fe^{3+}. As the temperature falls below 230 K, there is an initial increase in moment which is then reversed. This behaviour is probably indicative of an antiferromagnetic interaction with some misalignment of spins in the vicinity of the Néel temperature.

The Mössbauer spectra are shown in Figures 18 and 19. At 295 K the X component has intensified once again, and the computed figures for a 'thin' absorber and using the three-component model are as in Table 5. Although a good overall curve fit can be obtained, the model is probably least satisfactory for this sample because the Y component appears broad and ill defined. In particular, it is difficult to obtain reliable area ratios, and the values quoted could be in error by several percent. Once again the X component becomes magnetic below 220 K, but there is considerable asymmetric broadening of the central Y and Z components with decreasing temperature. The spectrum at 4.2 K is very similar to that for sample (**1b**) (Figure 10), but the magnetic Y components appear weaker.

It appears, therefore, that quench-cooling from 900 K in air can produce a material which is very similar to a slow-cooled sample re-annealed *in vacuo* at 700 K. Although quenching

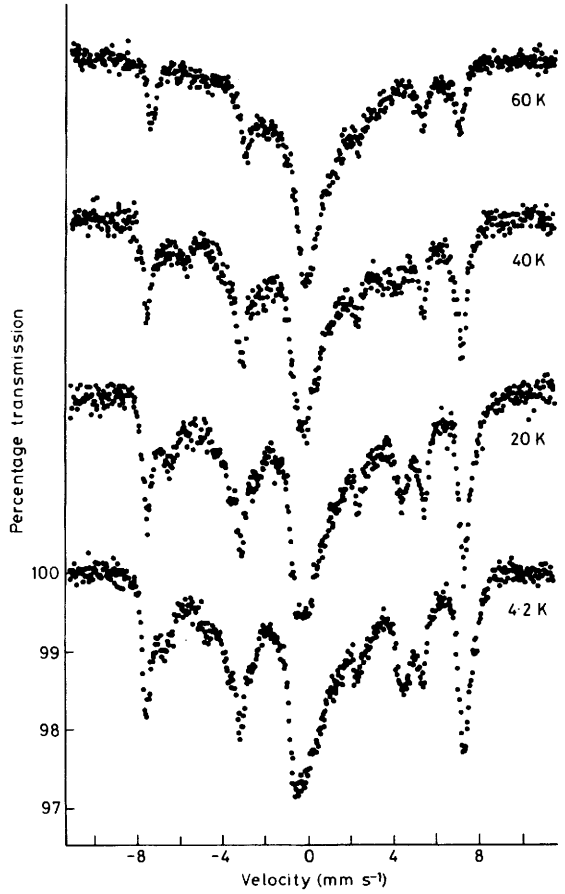

Figure 15. The ^{57}Fe Mössbauer spectrum of sample (**1c**) ($SrFeO_{2.846}$) at 4.2, 20, 40, and 60 K

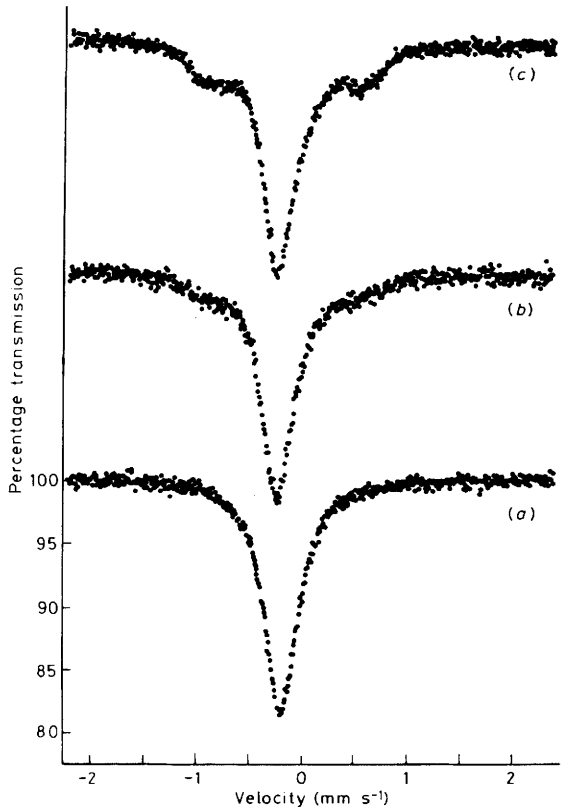

Figure 16. The ^{57}Fe Mössbauer spectrum of sample (**1a**) ($SrFeO_{2.844}$) *in vacuo* (*a*) at 800 (for 1 d), (*b*) at 900 (for 24 h), and (*c*) at 900 K (24—72 h). Note the emergence of new components at 900 K due to $SrFeO_{2.50}$

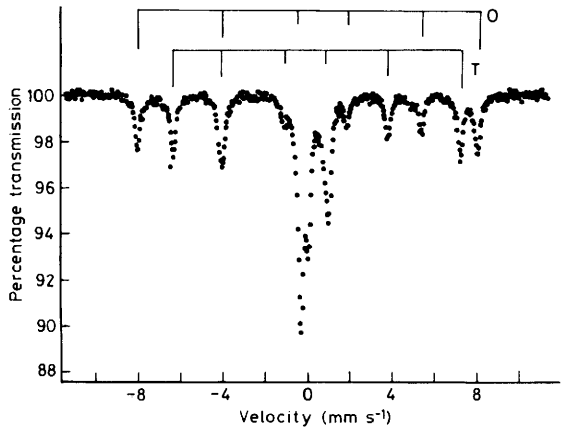

Figure 17. The ^{57}Fe Mössbauer spectrum of sample (**1e**) ($SrFeO_{2.589}$) at 295 K showing the two magnetic hyperfine patterns due to $SrFeO_{2.50}$. Fe^{3+} cations are in octahedral (O) or distorted tetrahedral (T) geometry

could in principle result in an inhomogeneous material, there was no real evidence to suggest that this was the case.

Sample (**2c**) ($SrFeO_{2.749}$).—An aliquot of sample (**2a**) was annealed *in vacuo* at 700 K for 5 d in an attempted repeat of the preparation of sample (**1b**). However, the longer heating time resulted in greater loss of oxygen than intended, and the susceptibility data shown in Figure 7(*c*) are similar to those for the quenched sample (**2b**).

Sample (**2d**) ($SrFeO_{2.804}$).—An aliquot of Sample (**2a**) was annealed at 1 570 K for 24 h and then cooled very slowly to 680 K at an average rate of *ca.* 3° h^{-1}. Surprisingly, the oxygen content was less than in the starting material, and this is confirmed by an increase in the intensity of the X component.

Sample (**2e**) ($SrFeO_{2.787}$).—Sample (**2d**) was reheated to 1 200 K and then cooled more quickly, reaching 750 K in 18 min. This reduced the oxygen content more than in the previous case, and the spectrum at 4.2 K showed very sharp lines for the X component.

Sample (**3**) ($SrFeO_{2.809}$).—A third preparation was carried out using only one heating cycle, *i.e.* without any annealing cycles as applied to (**1a**) and (**2a**). The oxygen content proved to be slightly lower in this sample, but the same general features are apparent in the spectra. It had been hoped that sample (**3**) would resemble the original preparation by Gallagher *et al.*[1] more closely, but no sample has been produced in the present work without an appreciable contribution from the X component.

Discussion

The data obtained have been described fully without any attempt to explain their full significance. This is partly because of the complexity of the problem, but mainly because of the need to examine the data as a whole in proposing an interpretation. Very few oxides are known which contain iron in higher oxidation states, and as the discussion will show, much of

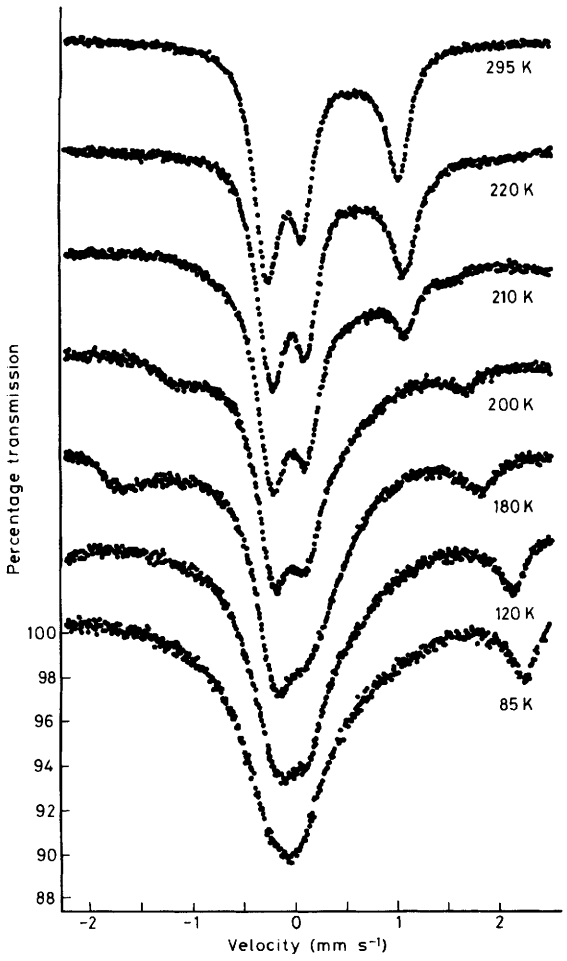

Figure 18. The ^{57}Fe Mössbauer spectra of sample (**2b**) ($SrFeO_{2.760}$) at 85, 120, 180, 200, 210, 220, and 295 K

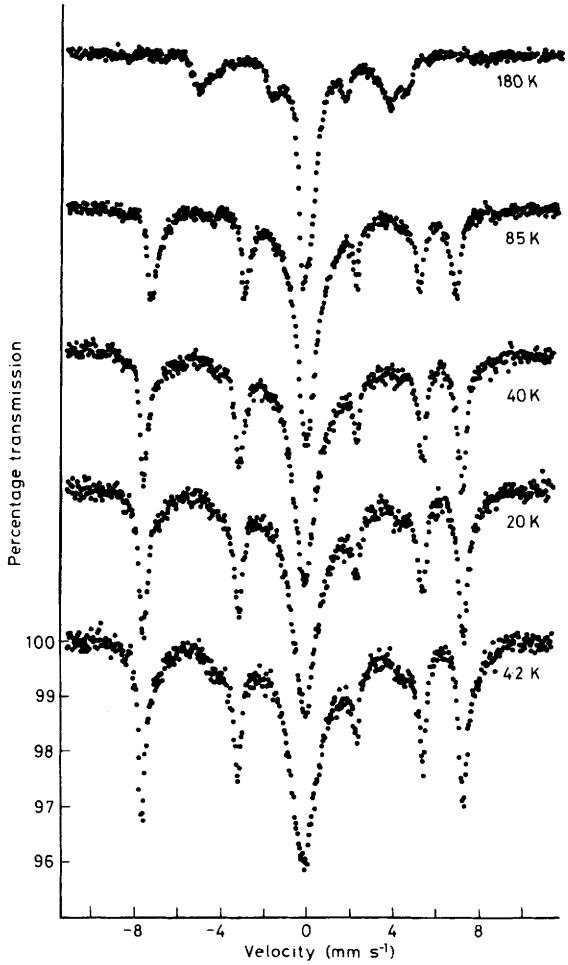

Figure 19. The ^{57}Fe Mössbauer spectra of sample (**2b**) ($SrFeO_{2.760}$) at 4.2, 20, 40, 85, and 180 K

the available information is incorrect, inadequate, or misleading in its interpretation.

The classic work [1,2] on $SrFeO_{3-y}$ concentrated mainly on the oxygen-rich materials made under very high partial pressures of oxygen. Stoicheiometric $SrFeO_3$ is a cubic perovskite with a cell constant $a = 3.850$ Å, is a metallic conductor, and orders antiferromagnetically below 134 K. The Mössbauer spectra show a single line at room temperature with an isomer shift of 0.054 mm s^{-1}, and a sharp magnetic hyperfine pattern at 4.2 K with a shift of 0.146 mm s^{-1} and a magnetic flux density of 33.1 T. There is no quadrupole effect. The magnetic flux density seems compatible with an octahedral d^4 ($t_{2g}^3 e_g^1$, $S = 2$) high-spin Fe^{4+} configuration with some degree of covalency, bearing in mind that d^5 ($S = \frac{5}{2}$) high-spin Fe^{3+} ions can show flux densities as low as 45 T. The value seems far too large to be due to a d^4 (t_{2g}^4, $S = 1$) low-spin Fe^{4+} configuration, as inferred from a neutron diffraction study.[6] The fact that no Jahn–Teller distortion occurs can be rationalized without invoking a low-spin configuration if, for example, the metallic conductivity arises from a delocalised σ^* band (derived from the e_g electron states), with a localised symmetrical half-filled t_{2g}^3 configuration. The paramagnetic moment of $SrFeO_3$ is anomalously high and not understood.[2]

Some physical properties have been reported [2] on $SrFeO_{3-y}$ for small values of y, and it is clear that the ordering temperature decreases and the resisitivity increases with increasing y. Unfortunately, corresponding Mössbauer data are not available.

Table 5. Calculated Mössbauer parameters for sample (**2b**)

Component	δ/mm s^{-1}	Δ/mm s^{-1}	Γ/mm s^{-1}	Area (%)
X	0.35	1.31	0.24	33
Y	0.36	0.64	0.63	22
Z	−0.08	0.30	0.25	45

A composition $SrFeO_{2.84}$ made from SrC_2O_4 and Fe_2O_3 with slow cooling in air [and potentially similar to sample (**1a**)] was a tetragonally distorted perovskite with a much larger resistivity. The magnetisation showed a sharp break at 80 K, and it was commented [2] that similar behaviour has been observed in other grossly defect compounds where defects can be ordered in certain planes by annealing at low temperatures. However, no other evidence for defect ordering was obtained.

As already observed, the Mössbauer spectra reported [1] for $SrFeO_{2.86}$ at 300, 78, and 4 K were similar to the new data, but without any reference to the X component. The overall interpretation was based on the assumption that the solid contains Fe^{3+} and Fe^{4+} cations and oxygen vacancies. The most intense component of Figure 1 was assigned to Fe^{4+} ($\delta = 0.021$ mm s^{-1} at 298 K), despite the anomalous second-order doppler shift which this implied. At 4 K the two magnetic flux densities (the Y and Z components) were given as 42.1 and 29.1 T for Fe^{3+} and

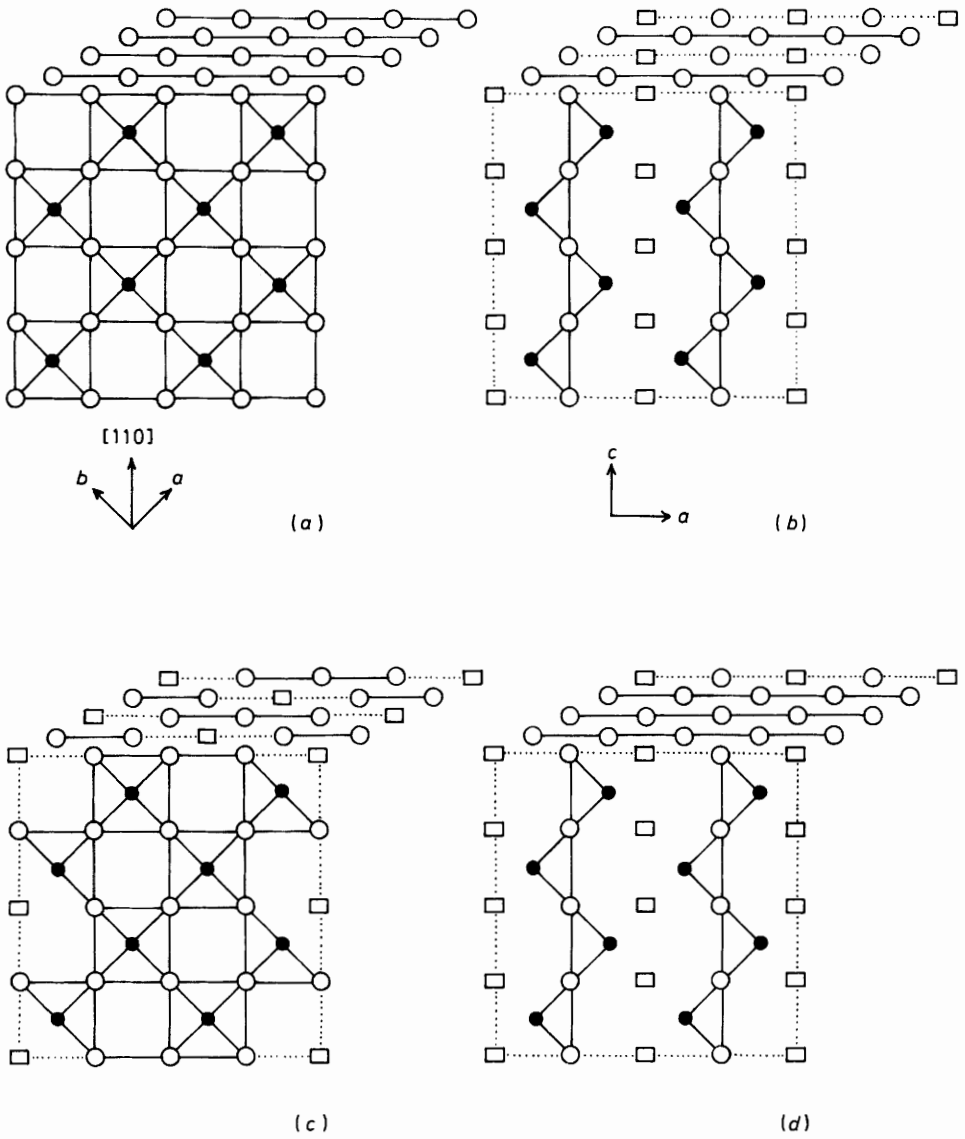

Figure 20. (*a*) The cubic perovskite structure of $SrFeO_3$, made up of corner-sharing FeO_6 octahedra, represented schematically as a projection on the (001) plane with the Sr atoms omitted. The edges of parallel (001) planes are represented by the parallel lines. (*b*) The structure of $SrFeO_{2.5}$: considerably distorted, but can be derived from that of $SrFeO_3$ by inserting strings of oxygen vacancies along the [110] axis. These strings then repeat in alternate (001) planes to give alternate layers of FeO_6 octahedra and FeO_4 distorted tetrahedra. (*c*) The previously proposed defect structure (ref. 8) for $SrFeO_{2.75}$, containing fewer defects, arranged in such a way that 50% of the Fe sites are six-co-ordinated and 50% are five-co-ordinated. (*d*) The structure proposed in the present work, showing a close similarity to $SrFeO_{2.5}$ but with layers of FeO_4 distorted tetrahedra separated by three layers of FeO_6 octahedra

Fe^{4+} respectively. The significance of the low value for Fe^{4+} compared to 33.1 T in $SrFeO_3$ was not deduced.

The perovskite solid solution $Sr_{1-x}La_xFeO_3$ is interesting in that substitution of La^{3+} into $SrFeO_3$ causes partial reduction of Fe^{4+} to Fe^{3+}, although the Sr-rich end of the phase also shows oxygen deficiency. Early Mössbauer measurements[3] showed evidence for only a single iron species at 295 K in the range $0.3 \leqslant x \leqslant 0.6$, and it was suggested that an 'intermediate' or averaged valency state existed. Two distinct species, described as Fe^{4+} and Fe^{3+}, were seen for $0 \leqslant x \leqslant 0.2$, although as indicated earlier, the evidence for an X component in $SrFeO_{2.841}$ was ignored.

Later work on $SrFeO_{3-y}$ using electron diffraction[8,9] found some evidence for a defect superstructure. Preparations of $SrFeO_{3-y}$ by direct reaction of $SrCO_3$ and Fe_2O_3 in air can lead to compositions up to $SrFeO_{2.87}$, while preparations from $SrFeO_{2.50}$ (itself made from $SrCO_3$ and Fe_2O_3) by oxygen uptake had a maximum oxygen content of $SrFeO_{2.78}$. This curious behaviour is supported by the present observation that prolonged annealing followed by slow cooling in air tended to reduce the oxygen content [*e.g.* samples (**2a**) and (**2d**)]. It is possible that this effect is related to non-thermodynamic defects such as grain boundaries which produce a major influence on the oxygen uptake and defect ordering in the lattice.

The electron diffraction data[8,9] gave conclusive evidence for a superstructure with an ideal composition presumed to be $SrFeO_{2.75}$ and a tetragonal or orthorhombic unit cell with dimensions $a \simeq 2\sqrt{2}\,a_c$, $b = 2\,a_c$, and $c = 2\sqrt{2}\,a_c$, where a_c is the cubic parameter of the $SrFeO_3$ lattice. The superstructure is not seen in the *X*-ray diffraction data, and this presumably is indicative of a very small microdomain structure which is only revealed by the shorter wavelength measurement.

The lattice of $SrFeO_{2.5}$ can be broadly related to the cubic perovskite (see Figure 20) by invoking an ordered array of

oxygen vacancies in strings along the [110] axis of the cubic cell such that alternate layers of the Fe atoms in the (001) planes are octahedrally and tetrahedrally co-ordinated to oxygen. A tentative structure for $SrFeO_{2.75}$ was proposed[8,9] in which every other oxygen is lost from certain strings such that half of the iron remains octahedrally co-ordinated and half becomes five-co-ordinated. Interestingly, a related structure has recently been derived from neutron diffraction data[15,16] for $CaMnO_{2.5}$ in which all the Mn^{3+} cations are five-co-ordinated in a nearly square-pyramidal geometry.

Reduction below $SrFeO_{2.75}$ seems to result in a mixture of $SrFeO_{2.5}$ and $SrFeO_{2.75}$, and intergrowth of these phases has been reported.[8] Thermogravimetric data[8] suggest that there is only a single phase in air between $SrFeO_{2.5}$ and $SrFeO_{2.75}$ in the temperature range 770—1 320 K where oxygen loss takes place. However, the two spectra recorded at 900 K *in vacuo* (Figure 16) in the present work give clear evidence that a phase separation takes place at this temperature. Heating at 700 K *in vacuo* for 5 d gave $SrFeO_{2.749}$ [sample (**2c**)], while quenching from 1 200 K gave $SrFeO_{2.760}$ [sample (**2b**)]. This is further evidence supporting the existence of a defect phase with the ideal composition $SrFeO_{2.75}$ (or $Sr_4Fe_4O_{11}$).

A room-temperature Mössbauer spectrum has been reported[9] for $SrFeO_{2.78}$ which appears very different to the data in Figures 9 and 18. It is not easy to comment further on this isolated result, other than to observe that the proposed interpretation invokes three types of iron: Fe^{4+}, and Fe^{3+} in both octahedral and tetrahedral co-ordination.

It is ironic that several of the features of the Mössbauer spectra of $SrFeO_{3-y}$ which are reported here have already been observed[17] in samples made by the thermal decomposition of the iron(VI) compound $SrFeO_4$. Unfortunately, no chemical analyses were reported, nor is the thermal treatment described in sufficient detail to allow a useful comparison.

The closely related iron(IV) compound, $CaFeO_3$, has been prepared comparatively recently[11,18] using high pressures of oxygen, and has thrown a completely new light onto the interpretation of compounds containing high oxidation states of iron. The structure appears to be a tetragonally distorted perovskite lattice. The high-temperature metallic-conducting paramagnetic phase undergoes an unusual phase transition below *ca.* 115 K to an antiferromagnetic semiconducting phase. This is in distinct contrast with $SrFeO_3$ which remains metallic at 4.2 K. At 300 K the Mössbauer spectrum of $CaFeO_3$ is a single line with an isomer shift of 0.073 mm s^{-1} [see point (2) in Figure 8]. However, at 4.2 K the spectrum comprises two superimposed magnetic hyperfine patterns, (a) and (b), of equal intensity and with the parameters given below. The isomer shift

	δ/mm s^{-1}	B/T
(a)	0.34	41.6
(b)	0.00	27.9
mean	0.17	34.8

values are plotted in Figure 8, and correspond almost exactly with those for the Y and Z components of $SrFeO_{2.844}$ obtained in the present work. The mean values for δ and B also correspond closely to the single values observed for stoicheiometric $SrFeO_3$. The spectrum at 77 K also shows two hyperfine patterns, but with some line broadening, possibly suggestive of valence fluctuation. These data were interpreted by a model in which the mobile electrons at high temperature, probably the e_g^* band, become localised at low temperature so as to effect the disproportionation (1).

$$2Fe^{4+} \rightleftharpoons Fe^{3+} + Fe^{5+} \quad (1)$$

This important observation has been subsequently qualified by other measurements which suggest that the disproportionation should really be written as in (2), where λ is a non-integral

$$2Fe^{4+} \rightleftharpoons Fe^{(4-\lambda)+} + Fe^{(4+\lambda)+} \quad (2)$$

increment. This interpretation is clearly indicated by the isomer shift and magnetic flux density values obtained[19] from the solid solution $Ca_{1-x}Sr_xFeO_3$ ($0 \leqslant x \leqslant 0.75$). These cubic perovskite solid solutions show asymmetric broad lines at room temperature, and become antiferromagnetic below 115—140 K. Two sharp hyperfine patterns are seen at 4.2 K with values for δ and B which interpolate almost linearly between the values for $CaFeO_3$ and $SrFeO_3$. Because the local atomic environment in a random solid solution will be non-uniform, the Mössbauer spectrum of an oxide with localised electron states normally shows multiple hyperfine patterns due to the different near-neighbour environments. This is clearly not the case in $Ca_{1-x}Sr_xFeO_3$, where the large variation in the observed parameters with composition seems to indicate the band-like nature of the electronic states and two apparent non-integral valence states. In $CaFeO_3$ itself, it seems reasonable to associate the field of 41.6 T with the state $Fe^{(4-\lambda)+}$ because this state could be expected to show both a larger unpaired spin density and a more positive chemical shift.

Returning for the moment to $SrFeO_{3-y}$, it can be seen that the Z component shows values of B = 29.3 T and δ = 0.03 mm s^{-1} which are fairly close to those for the $Fe^{(4+\lambda)+}$ component of $CaFeO_3$, *i.e.* we may well be seeing non-integral valence states in this phase. This could also explain why the isomer shift of the Z component is more negative than that of $SrFeO_3$ itself, but considerably more positive than the value of $\delta = -0.41$ mm s^{-1} at 293 K recorded[13] for the six-co-ordinate Fe^{5+} ion in La_2LiFeO_6 [see point (4) in Figure 8]. The latter compound becomes antiferromagnetic below T_N = 14.5 K, and shows a magnetic hyperfine splitting with B = 23.6 T, a value which seems reasonable for a (t_{2g}^3, $S = \frac{3}{2}$) configuration with considerable covalency.

Preliminary data for the fully oxidised solid solutions $Ca_{1-x}Sr_xFeO_3$ and $Sr_{1-x}La_xFeO_3$ seem to indicate[20] that the charge disproportionation takes place in both cases below the Néel temperature. Subsequent work[21] has shown that the two hyperfine components at 4.2 K produce an excellent correlation between the isomer shift and the flux density which is a universal curve for both solid solutions, and demonstrates convincingly the continuous variation in these parameters and the existence of effectively non-integral valence states. The observed values range from δ = 0.44 mm s^{-1}, B = 54.2 T to $\delta = -0.05$ mm s^{-1}, B = 26.6 T, and correlate extremely well with $SrFeO_3$ itself. The averaged values from the two components at any given composition also correlate with $SrFeO_3$. The detailed interpretation of the data appears fully consistent with the formulations given below. Unfortunately, the structural implications of this charge disproportionation have not been investigated.

$$Ca_{1-x}Sr_xFe^{(4-\lambda)+}{}_{0.5}Fe^{(4+\lambda)+}{}_{0.5}O_3$$

$$Sr_{1-y}La_yFe^{(4-\lambda)+}{}_{(1+y)/2}Fe^{(4+\lambda)+}{}_{(1-y)/2}O_3$$

In $Sr_{0.7}La_{0.3}FeO_3$ it was observed that considerable collapse of the hyperfine splitting occurred well below the ordering temperature. This was claimed to signify the coexistence of the paramagnetic averaged-valence phase and the antiferromagnetic mixed-valence phase. However, it seems more likely that what is seen is a relaxational collapse due to spin fluctuations.

Data are also available[22] for the solid solution $La_{1-x}Ca_xFeO_{3-y}$ ($0 \leqslant x \leqslant 0.5$, $0 \leqslant y \leqslant 0.07$). These materials are essentially antiferromagnetic semiconductors. Although the

conductivity is generally very small at low temperatures indicating localised electrons, it becomes appreciable at room temperature. The Mössbauer spectrum of $La_{0.50}Ca_{0.50}FeO_{2.93}$ at 293 K is a single broad slightly asymmetric line with a shift of $\delta = 0.20$ mm s^{-1}, and can be interpreted as a partially averaged spectrum due to electron hopping between Fe sites. Samples with $x = 0.2$, 0.3, and 0.5 at 4.2 K show three superimposed magnetic hyperfine patterns. The parameters show little dependence on composition, and the averaged values are given below. Components (i) and (j) were assigned to Fe^{3+}

	δ/mm s^{-1}	B/T
(i)	0.49	55
(j)	0.46	52
(k)	−0.07	27

cations with one and two Fe^{5+} nearest-neighbour cations respectively, and (k) was assigned to Fe^{5+} cations. The area ratios computed from the spectra agreed very well with the estimated values from the chemical formulae. The proposed model for the low-temperature state is of $t_{2g}^3e_g^2$ Fe^{3+} and $t_{2g}^3e_g^0$ Fe^{5+} cations in octahedral co-ordination.

If the values for δ and B for the (i), (j), and (k) components are compared to those for $SrFeO_{2.844}$ in Figure 8, it is immediately apparent that the δ value for the (k) component is substantially more negative than that of the Z component. Similarly, the flux density B (*ca.* 27 T) is less than the value of 29.3 T seen in Figure 6. The δ values for the (i) and (j) Fe^{3+} components are also substantially more positive than for the X and Y components, and the values for B are also substantially greater. Therefore, one can deduce that the *d*-electron spin density at the various cation sites in $SrFeO_{3-y}$ appears to be intermediate between the two extremes of Fe^{3+} and Fe^{5+}.

It has been claimed[22] that the lower shift and flux density recorded for Fe^{5+} in La_2LiFeO_6 compared to $La_{1-x}Ca_xFeO_{3-y}$ reflect the greater covalency of the Fe–O bond in the former caused by the more ionic antagonistic Li–O bond. A similar effect has been noted[23] in $SrLa_3LiFeO_8$ which is a nominal Fe^{4+} oxide with the K_2NiF_4 structure, distorted octahedral co-ordination about the iron, and a network of Fe–O–Li bonds. The observed paramagnetic moment of 4.95 B.M. is consistent with high-spin Fe^{4+}, and the d^4 configuration would be expected to show a Jahn–Teller distortion which is presumably the origin of the large quadrupole splitting. The value of $\delta = -0.18$ mm s^{-1} at 290 K is substantially lower than in $SrFeO_3$. The flux densities at 4.2 K ($T_N = 29.7$ K) for the two different sites are only 15.3 and 13.1 T, but an anisotropic electron configuration results in additional contributions to the total flux density which are difficult to estimate exactly. However, differences caused by such covalency effects should be much less in $SrFeO_3$, $CaFeO_3$, and $La_{1-x}Ca_xFeO_{3-y}$, and the available data seem consistent with this view.

Before attempting to explain the new data for $SrFeO_{3-y}$ more fully, it is worth reflecting on the different electronic states for a mixed-valence iron compound which might exist: (*i*) Fe atoms with *localised* electrons and *integral* charges, *i.e.* a mixture of conventional ions which could be Fe^{3+}, Fe^{4+}, or Fe^{5+}; (*ii*) Fe atoms with fully *delocalised* electrons at all temperatures as seen for example in stoicheiometric $SrFeO_3$; (*iii*) two or more distinct localised ionic states (*e.g.* Fe^{3+}/Fe^{4+}, Fe^{3+}/Fe^{5+}, *etc.*) which appear *static* at low temperatures but exchange an electron at higher temperatures to give an '*averaged*' valence state (this possibly pertains to the $La_{1-x}Ca_xFeO_{3-y}$ phase); (*iv*) two distinct types of atom which are both involved in a *delocalised* electron system but are at chemically different sites so that they can be represented by *non-integral* charge states $Fe^{(n+\alpha)+}$ and $Fe^{(n+\beta)+}$; it seems likely that the charge disproportionation in $CaFeO_3$ and $Ca_{1-x}Sr_xFeO_3$ is of this type.

Table 6. Percentages of the components determined from the spectra with those calculated from the formulae for samples (**1a**), (**1b**), (**1c**), and (**2b**)

Sample	X	Y	Z	Fe^{3+}	Fe^{4+}	Fe^{3+}	Fe^{5+}
(**1a**) $SrFeO_{2.844}$	9	45	46	31	69	66	34
(**1b**) $SrFeO_{2.808}$	30	20	50	38	62	69	21
(**1c**) $SrFeO_{2.846}$	18	33	49	31	69	65	35
(**2b**) $SrFeO_{2.760}$	33	22	45	48	52	74	26

It has already been shown that the spectra for $SrFeO_{3-y}$ can, in general, be interpreted in terms of three components X, Y, and Z, the only potential problem occurring with the quenched sample (**2b**) where the Y component is broadened. The area ratios for samples (**1a**), (**1b**), (**1c**), and (**2b**) cannot be interpreted simply in terms of integral charge states. If X and Y are considered to be two different types of Fe^{3+}, and Z is either Fe^{4+} or Fe^{5+}, then the percentages of the three components by area and the ideal percentages calculated from the chemical formulae are as in Table 6. Even allowing for some difference in recoilless fractions, it is clear that the Z component is unlikely to be simply Fe^{4+} or Fe^{5+}. This rules out a simple localised model of type (*i*) or (*iii*).

The X Component.—The increase in intensity of the X component with increasing oxygen deficiency, and also with annealing [samples (**1a**), (**1c**)], suggests strongly that it is related to the oxygen vacancies which are present. The large quadrupole splitting which shows little variation could be indicative of a highly distorted but consistent environment for a proportion of the Fe atoms. The isomer shift is typical of the Fe^{3+} oxidation state, which is an *S*-state ion (d^5) with no intrinsic valence contribution to the quadrupole splitting. A simple point-charge calculation ignoring all covalency effects for an Fe^{3+} site with an oxygen vacancy (and a virtual charge of $+2e$) at a distance of 193 pm gives a value for the expected quadrupole splitting, $\Delta = e^2qQ/2$, of +3.16 mm s^{-1}. On the other hand, two oxygen vacancies at adjacent corners of an otherwise undistorted octahedral site would give a splitting of −3.16 mm s^{-1}. Allowing some relaxation of the remaining oxygen positions markedly affects the magnitude of the predicted splitting, but the sign can only be altered by very severe and perhaps unlikely distortions. However, simple lattice calculations are not always successful in predicting the correct quadrupole splitting, and it should be borne in mind that the reasonably symmetrical six-co-ordinated site in $SrFeO_{2.5}$ shows an unexpectedly large splitting.

In magnetic hyperfine spectra showing a simultaneous quadrupole perturbation, the relative orientation of the magnetic axis and the electric field gradient tensor is implicitly contained in the perturbation parameter ε, but in general the problem is underdetermined so that a range of possible solutions can be defined. A general analysis for the ^{57}Fe spectrum has been described in detail.[24] The spectra for sample (**2b**) show the best resolution of the X component, and at 4.2 K give a quadrupole perturbation parameter of $\varepsilon = -0.619$ mm s^{-1}, and at 295 K gave a quadrupole splitting of $|\Delta| = 1.311$ mm s^{-1}. Assuming that Δ is independent of temperature, the ratio $|R| = 2\varepsilon/\Delta = 0.94$ can be compared with the graphs of Caër *et al.*[24] to establish that the value of R can only have a positive sign, and therefore that the quadrupole splitting is in fact -1.311 mm s^{-1}. Furthermore, the angle θ between the principal axis of the electric field gradient and the direction of the magnetic field lies in the range $0 \leqslant \theta \leqslant 12°$, and the asymmetry parameter η lies in the range $0 \leqslant \eta \leqslant 0.6$. These deductions appear to be valid for the X component in all samples regardless of composition.

The negative sign of the quadrupole splitting is totally inconsistent with a single oxygen vacancy in the ideal octahedral co-ordination about the iron, but could be rationalised with distorted four-co-ordination. It also appears that the principal axis of the electric field gradient and the magnetic field are almost collinear.

Although $SrFeO_{2.5}$ and $CaFeO_{2.5}$ show slight structural differences, these are relatively minor.[7,25] The Mössbauer spectra are very similar indeed. A detailed analysis of the magnetic spectra for $CaFeO_{2.5}$ has shown[26] that the quadrupole splitting from the tetrahedral site iron has a negative sign, and that while the principal value of the electric field gradient lies along the *b* axis of the crystal, the magnetic hyperfine field lies along the *c* axis, *i.e.* the two axes are perpendicular to each other, and that η is <0.4.

The lines from $SrFeO_{2.5}$ in the spectrum of sample (**1e**) in Figure 17 have been assigned to the tetrahedral and octahedral sites by analogy with $CaFeO_{2.5}$. The perturbation parameter ε for the tetrahedral site is $\varepsilon = +0.289$ mm s^{-1}. Assuming that $\eta \simeq 0$ and using the standard formula for $\varepsilon = (e^2qQ/8)(3\cos^2\theta - 1)$ with $\theta = 90°$, the expression $\Delta = e^2qQ/2 = -1.16$ mm s^{-1} is obtained. This value is very close to that of component X. If the spin axis were rotated to lie along the *b* axis collinear with the electric field gradient, *i.e.* the spins are perpendicular to the (001) plane shown in Figure 20(*b*), then the two spectra would be almost identical. It is considered that this is strong evidence for associating the component X with layers of Fe^{3+} cations in a distorted tetrahedral co-ordination very similar to that found in $SrFeO_{2.5}$.

As a general rule the isomer shift for an Fe^{3+} ion in six-co-ordination is more positive than for an Fe^{3+} ion in four-co-ordination because of an increase in covalency in the bonding. The isomer shift at 4.2 K of component X in sample (**1a**) of $+0.43$ mm s^{-1} is smaller than the average value of $+0.49$ mm s^{-1} found in $La_{1-x}Ca_xFeO_{3-y}$ for octahedrally co-ordinated Fe^{3+} ions, and is, therefore, consistent with a lower co-ordination number. However, the isomer shift at 295 K is almost identical to that found in the solid solution $EuFe_{0.5}Co_{0.5}O_3$ (see Figure 8) where the co-ordination of the iron is six, and is much closer to the shift found in $SrFeO_{2.5}$ for six-co-ordination. It is possible that the temperature dependence of the isomer shift from the X component in $SrFeO_{2.844}$ is anomalous because of the thermally activated electron-exchange process which takes place at higher temperatures.

One of the more unusual aspects of this strontium ferrate phase is the way in which the X component shows a magnetic hyperfine splitting below *ca.* 220 K apparently independent of the percentage of this component in the spectrum (9—33%) within the composition range $SrFeO_{2.844-2.760}$. Moreover, all the experimental evidence points to the samples being single phase. One interpretation which can explain many of the facts is to propose the existence of a planar defect of oxygen vacancies in the (001) plane, forming a layer of Fe^{3+} cations with distorted four-co-ordination and localised electrons, very similar to the layers in $SrFeO_{2.5}$, but with the spin axis normal to the layers. If long-range magnetic order can occur in two dimensions within these layers, but not within the intervening layers (for reasons to be discussed later), then the critical temperature will be nearly independent of the weaker interactions with other such layers at large and perhaps irregular spacings.

Is such a model realistic? A recent highly detailed study[27] of the critical behaviour in the layered antiferromagnet $KFeF_4$ had confirmed the existence of long-range order in only *two* dimensions in this compound. The magnetic behaviour of highly anisotropic materials is governed by both the exchange anisotropy and the magnetic anisotropy of the spin system. In layered materials the interlayer exchange interaction can be much weaker than the intralayer exchange. If the magnetic anisotropy which derives from crystal-field effects is isotropic (Heisenberg magnet) or two-dimensional (*XY* magnet), then long-range ordering cannot take place. It is only in the particular case of a uniaxial magnetic anisotropy (Ising magnet) that long-range order is theoretically allowed. In the case of $KFeF_4$ the spins are aligned perpendicular to the antiferromagnetic layers because of this. Therefore, it can be concluded that two-dimensional long-range order is an established phenomenon. However, although the exchange anisotropy may be large in a layer structure, the weak interlayer coupling may still be sufficient to produce a three-dimensional long-range order as seen, for example,[27] in the very similar compound $RbFeF_4$. Unfortunately, the nature of the present system precludes any study of the critical phenomena near the ordering temperature and, hence, a direct determination of the dimensionality. However, the observation that the Fe^{3+} spins are aligned perpendicular to the four-co-ordinate layers is fully consistent with a two-dimensional Ising magnet, and may, therefore, be highly significant.

In sample (**1a**) ($SrFeO_{2.844}$) the X component is only 9% of the spectrum by area compared to a maximum concentration of 15.6% if all the oxygen vacancies aggregate into these postulated layers. Annealing at 700 K in air to give sample (**1c**) ($SrFeO_{2.846}$) increases the X component to 18% by area which is consistent with a *nearly complete ordering of the vacancies.* However, the agreement is less satisfactory for samples (**1b**) ($SrFeO_{2.808}$) and (**2b**) ($SrFeO_{2.760}$) where the maximum theoretical concentrations of 19.2 and 24.0% are in poor agreement with the observed areas (from 'thin' absorbers) of 30 and 33% respectively.

A correction for saturation would reduce these figures slightly, but the discrepancy still seems to be larger than one would reasonably expect to arise from differences in the recoilless fractions of the three components. Texture or preferred orientation in an absorber can also produce asymmetry in the quadrupole spectrum, but the absorbers were normally made by grinding with an excess of MgO as a diluent, and no evidence was found for orientation effects. A likely solution to the problem can be obtained by examining the spectra for samples (**1a**), (**1b**), (**1c**), and (**2b**) in Figures 4, 9, 13, and 18. In samples (**2a**) and (**1c**) the Y component remains a well defined doublet. In samples (**1b**) and (**2b**) the Y component is much broader and less well defined, and the use of symmetrical Lorentzian profiles in the area analysis is almost certainly unjustified. It seems probable that the constrained curve-fitting procedure will give a reasonably accurate area for component Z, because of the large difference in shift, but will be less than adequate in separating the X and Y components which have a similar shift and will therefore be more interactive. It seems possible that the idealized composition $SrFeO_{2.75}$ corresponds to the ratios of 1:1:2 for X:Y:Z.

The tendency to show inward relaxational collapse of the X magnetic hyperfine splitting with rise in temperature is probably associated with various imperfections in the layers such as incomplete defect ordering and microdomain boundaries. It is not unreasonable that this should be most marked in the original sample (**1a**) where only about half the oxygen vacancies have aggregated into complete layers.

There is substantial evidence for the existence of similar defect layers in other related oxides. Thus, in the perovskite solid solution $Ca_2Fe_{2-2x}Ti_{2x}O_{5+x}$ where $0 < x < 0.45$, electron microscope and Mössbauer data[28,29] have provided direct evidence for the existence of isolated layers of FeO_4 distorted tetrahedra separated by layers of MO_6 octahedra containing Fe^{3+} and Ti^{4+}. Materials with one, two, and three interleaved layers of octahedra were positively identified, as well as a more complex structure with an alternation of one and two layers of octahedra. These phases can be regarded as an intergrowth of

the perovskite and brownmillerite ($CaFeO_{2.5}$) type lattices, and provide an interesting method of incorporating large variations in composition in a structure with a fairly ordered lattice. In compositions close to $CaTiO_3$ the oxygen vacancies are more random. However, FeO_4 tetrahedra are still observed, and show a large quadrupole splitting which is not very sensitive to the composition.

In the reduced phase $La_{1-2x}Ca_{2x}FeO_{3-x}$ which contains only Fe^{3+} the existence of tetrahedral sites has been confirmed[30] for x values as small as 0.10. Long-range order involving planar defect arrays are observed for $x > 0.22$. Electron micrographs of oxidized samples containing Fe^{4+} in the phase $La_{1-x}Ca_xFeO_{3-y}$ have shown[31] the existence of a microdomain texture in which the $CaFeO_{2.5}$ lattice is intergrown with a $Ca_2LaFe_3O_8$ substructure which has layers of tetrahedra separated by two layers of octahedra. The *X*-ray powder data show a cubic lattice, and give no clue to the real structure. A microdomain texture has also been reported[32] in the reduced phase $Nd_{1-2x}Sr_{2x}FeO_{3-x}$, where the *X*-ray diffraction pattern is also cubic.

Against this background it seems highly probable that component X is indeed produced by a two-dimensional layer of Fe^{3+} cations in distorted tetrahedral co-ordination.

The Y and Z Components.—The aggregation of the oxygen vacancies into layers is essentially complete in annealed samples such as (**1b**), (**1c**), and (**2b**), and therefore the Y and Z components in these samples are from Fe atoms without an adjacent oxygen vacancy and with near-octahedral co-ordination to oxygen. In samples with a high oxygen content such as (**1a**), (**1d**), and (**2a**), some 30—40% of the oxygen vacancies must occur in a more random distribution, but apparently do not produce a large electric field gradient at near-neighbour iron atoms.

A significant feature of the data is that the area of the Z component is always close to 50% of the total area of the spectrum. In an ideal composition $SrFeO_{2.75}$ the maximum contribution from the tetrahedral Fe^{3+} ions of X is 25%, leaving a contribution of 25% from Y. A structure can be conceived in which the sequence of octahedral (O) and tetrahedral (T) layers is regular, with a repeat arrangement of TOOO, *i.e.* three octahedral layers between tetrahedral layers. However, all octahedral layers are not equivalent as some share oxygens with two adjacent octahedral and one tetrahedral layer. The sequence TOOO is thus compatible with the assignment XZYZ, and is illustrated in Figure 20. Extra oxygen can be incorporated into the lattice by inserting into additional layers to give some XZYZYZ sequences, *etc.* A nominal charge assignment for Z of Fe^{4+} would require that Y in $SrFeO_{2.75}$ be Fe^{3+}. At first sight this is completely inconsistent with the data for $CaFeO_3$ at 4.2 K which show two shifts and hyperfine splittings almost identical to those of X and Y in sample (**1a**) (Figure 8). These two components in $CaFeO_3$ have been interpreted in terms of the charge states $Fe^{(4-\lambda)+}$ and $Fe^{(4+\lambda)+}$. In $SrFeO_{2.75}$ the oxygen deficiency limits the charge states to a maximum of 50% 'Fe^{4+}', and it is not easy to understand the significance of the chemical shift of Z, which is substantially lower than that of $SrFeO_3$.

At this juncture it is appropriate to examine the magnetic susceptibility data in Figure 7 in more detail. The average paramagnetic moment for sample (**1a**) ($SrFeO_{2.844}$) is *ca.* 4.7 B.M. per iron atom above 230 K, which is lower than the spin-only values of 5.92 (for Fe^{3+}, $S = \frac{5}{2}$) and 4.90 B.M. (for high-spin Fe^{4+}, $S = 2$). Furthermore, the average moment for sample (**2b**) ($SrFeO_{2.760}$) is only *ca.* 3 B.M. above 230 K. Even the hypothetical configuration of 50% Fe^{3+} ($S = \frac{5}{2}$) and 50% low-spin Fe^{4+} ($S = 1$) would give an average moment of *ca.* 4.37 B.M. It is quite clear that the observed moment is very low and completely inconsistent with any combination of possible spin states for iron cations with formal charges of +3, +4, and +5.

It can also be asked why the Y and Z components do not show a static long-range magnetic order even at 4.2 K when the X component orders below 220 K. This behaviour is most unexpected. There is no reason to suspect that the d^4–d^5 magnetic exchange is exceptionally weak.

One possible interpretation is to assume a delocalisation of electrons in two dimensions in the octahedral layers. This cannot be simply a charge hopping between Fe^{3+} and Fe^{4+} cations, as such a process is usually thermally activated, and a freezing out of the individual ions at low temperature would be expected. Such behaviour is indeed seen near 600 K when electron exchange involving the tetrahedral layers also begins to take place. However, the Y and Z components appear to retain their identity right down to 4.2 K. On the other hand, a fully delocalised band system in two dimensions could approximate to a metal in character, and would not show any freezing out of charge states. Such a delocalised band would also tend to reduce any quadrupole behaviour substantially. If the layer plane is defined to be *xy*, then the $d_{x^2-y^2}$ and d_{z^2} orbitals, which contain either zero or one electron each, are those which contribute to the band structure. The d_{z^2} band would be narrow in energy and perhaps superimposed on a much broader $d_{x^2-y^2}$ band so that the Fermi surface consists of electron states in the *xy* plane. It seems reasonable to postulate that a reduction in the paramagnetic moment would result. The bulk conductivity need not be very sensitive to this delocalisation if microdomains exist which 'block' the layer conduction.

The existence of delocalised electron states could also provide an explanation for the failure to produce static magnetic interaction within the layers. However, in the present materials it is difficult to distinguish between a genuine time-dependent phenomenon and an inhomogeneous behaviour in which several distinct contributions are superimposed. It should be noted that sites Y and Z can both belong to a delocalised system, but are chemically distinct because of a differing environment and show different isomer shifts. The anisotropic nature of the electronic delocalisation may have an unusual effect on the isomer shifts. The partial development of a hyperfine splitting from Y and Z at low temperatures in sample (**1a**) for example may be the result of the increased disorder in this sample with substantial transfer of oxygen vacancies into the Y layers. This will have a major influence on the delocalised system, producing a narrower band of electron states and increasing the number of strongly interacting localised electron configurations. Against this background, it is difficult to make a detailed analysis of the isomer shift data. The reported correlation between flux density and isomer shift[21] in $Ca_{1-x}Sr_xFeO_3$ and $Sr_{1-x}La_xFeO_3$ is not necessarily applicable to the partially reduced phases. The noticeable decrease in isomer shift of Z with decreasing oxygen content is unlikely to signify an increase in the effective oxidation state, but could be the result of a modification to the electron states by more effective delocalisation in the idealised $SrFeO_{2.75}$.

The model which has been developed does provide a convenient explanation of the absence of a solid solution for $y > 0.28$. If one additional tetrahedral layer is inserted into a TOOOTOOOTOOO sequence, the resulting TOOO(OTOTOTO)OO sequence contains no less than *seven* layers in the correct sequence for $SrFeO_{2.5}$. It seems reasonable, therefore, to assume that intergrowth of $SrFeO_{2.75}$ and $SrFeO_{2.5}$ or even complete disproportionation will readily occur.

Conclusions

It has been firmly established that samples in the phase $SrFeO_{3-y}$ ($0.15 < y < 0.25$) are single-phase perovskites, but

depending on their thermal history may show a high degree of ordering of the oxygen vacancies. It is believed that the vacancies aggregate into (001) layers such that Fe^{3+} cations in distorted tetrahedral co-ordination are formed. The magnetic properties of these materials are very unusual, and suggest the existence of two-dimensional long-range order within the tetrahedral (T) layers. It is tentatively proposed that electron delocalisation can occur in the intervening layers with iron atoms in octahedral (O) co-ordination, and that the idealised structure $SrFeO_{2.75}$ contains the sequence TOOO. Insertion of further oxygen vacancies into this structure can lead logically to the observed disproportionation which occurs for $y > 0.28$.

The present work has used Mössbauer spectroscopy as a microscopic technique to probe individual atomic environments, and has revealed much new information about the defect structure. The phase is clearly extraordinary in its electronic properties, and this has prompted the full description of the data in this paper. However, many questions still remain, and the interpretation presented here may not be correct in all respects. It is unfortunate that the compounds lose oxygen so readily, and therefore preclude the use of electron microscope imaging techniques. However, neutron diffraction measurements at low temperature should prove interesting, and it is proposed to initiate work in this direction in the near future.

Acknowledgements

I am grateful to Mr. A. Hedley for the analyses, to Dr. A. Earnshaw for the magnetic susceptibility data, and to the S.E.R.C. for financial support.

References

1 P. K. Gallagher, J. B. MacChesney, and D. N. E. Buchanan, *J. Chem. Phys.*, 1964, **41**, 2429.
2 J. B. MacChesney, R. C. Sherwood, and J. F. Potter, *J. Chem. Phys.*, 1965, **43**, 1907.
3 U. Shimony and J. M. Knudsen, *Phys. Rev.*, 1966, **144**, 361.
4 P. K. Gallagher, J. B. MacChesney, and D. N. E. Buchanan, *J. Chem. Phys.*, 1966, **45**, 2466.
5 T. Takeda, Y. Yamaguchi, and H. Watanabe, *J. Phys. Soc. Jpn.*, 1972, **33**, 967.
6 H. Oda, Y. Yamaguchi, H. Takei, and H. Watanabe, *J. Phys. Soc. Jpn.*, 1977, **42**, 101.
7 C. Greaves, A. J. Jacobson, B. C. Tofield, and B. E. F. Fender, *Acta Crystallogr., Sect. B*, 1975, **31**, 641.
8 B. C. Tofield, C. Greaves, and B. E. F. Fender, *Mater. Res. Bull.*, 1975, **10**, 737.
9 B. C. Tofield, Proceedings of 8th International Symposium on Reactivity of Solids, eds. J. Wood, O. Lindqvist, and C. Helgesson, Plenum, New York, 1977.
10 P. K. Gallagher, J. B. MacChesney, and D. N. E. Buchanan, *J. Chem. Phys.*, 1965, **43**, 516.
11 M. Takano, N. Nakanishi, Y. Takeda, S. Naka, and T. Takada, *Mater. Res. Bull.*, 1977, **12**, 923.
12 B. Buffat, G. Demazeau, M. Pouchard, L. Fournès, J. M. Dance, P. Fabritchnyi, and P. Hagenmuller, *C.R. Hebd. Seances Acad. Sci., Ser. 2*, 1981, **292**, 509.
13 G. Demazeau, B. Buffat, F. Ménil, L. Fournès, M. Pouchard, J. M. Dance, P. Fabritchnyi, and P. Hagenmuller, *Mater. Res. Bull.*, 1981, **16**, 1465.
14 F. K. Lotgering and A. M. van Diepen, *J. Phys. Chem. Solids*, 1977, **38**, 565.
15 K. R. Poepplmeier, M. E. Leonowitz, and J. M. Longo, *J. Solid State Chem.*, 1982, **44**, 89.
16 K. R. Poepplmeier, M. E. Leonowitz, J. C. Scanlon, and J. M. Longo, *J. Solid State Chem.*, 1982, **45**, 71.
17 T. Ichida, *Bull. Chem. Soc. Jpn*, 1973, **46**, 1591.
18 Y. Takeda, S. Naka, M. Takano, T. Shinjo, T. Takada, and M. Shimada, *Mater. Res. Bull.*, 1978, **13**, 61.
19 Y. Takeda, S. Naka, and M. Takano, *J. Phys. (Paris), Colloq. C2*, 1979, **40**, C2-331.
20 M. Takano, N. Nakanishi, Y. Takeda, and S. Naka, *J. Phys. (Paris), Colloq. C2*, 1979, **40**, C2-313.
21 M. Takano, J. Kawachi, N. Nakanishi, and Y. Takeda, *J. Solid State Chem.*, 1981, **39**, 75.
22 S. Komornicki, L. Fournès, J. C. Grenier, F. Ménil, M. Pouchard, and P. Hagenmuller, *Mater. Res. Bull.*, 1981, **16**, 967.
23 M. F. Thomas, G. Demazeau, M. Pouchard, and P. Hagenmuller, *Solid State Commun.*, 1981, **39**, 751.
24 G. Le Caër, J. M. Dubois, L. Häggström, and T. Ericsson, *Nucl. Instrum. Methods*, 1978, **157**, 127.
25 E. F. Bertaut, P. Blum, and A. Sagnières, *Acta Crystallogr.*, 1959, **12**, 149.
26 R. W. Grant, *J. Chem. Phys.*, 1969, **51**, 1156.
27 H. Keller and I. M. Savic, *Phys. Rev. B*, 1983, **28**, 2638.
28 J. C. Grenier, G. Schiffmacher, P. Caro, M. Pouchard, and P. Hagenmuller, *J. Solid State Chem.*, 1977, **20**, 365.
29 J. C. Grenier, F. Ménil, M. Pouchard, and P. Hagenmuller, *Mater. Res. Bull.*, 1978, **13**, 329.
30 J. C. Grenier, L. Fournès, M. Pouchard, P. Hagenmuller, and S. Komornicki, *Mater. Res. Bull.*, 1982, **17**, 55.
31 M. A. Alario-Franco, J. M. Gonzalez-Calbet, M. Vallet-Regi, and J. C. Grenier, *J. Solid State Chem.*, 1983, **49**, 219.
32 M. A. Alario-Franco, J. C. Joubert, and J. P. Levy, *Mater. Res. Bull.*, 1982, **17**, 733.

Received 20*th September* 1984; *Paper* 4/1629